SCIENTIFIC COMMITTEE
TWELFTH REGULAR SESSION

Bali, Indonesia
3–11 August 2016

Predicting skipjack tuna dynamics and effects of climate change using SEAPODYM with fishing and tagging data

WCPFC-SC12-2016/EB WP-01

Inna Senina[1], Patrick Lehodey[1], Beatriz Calmettesa[1], Simon Nicol[2 3], Sylvain Caillot[2], John Hampton[2], and Peter Williams[2]

[1] Marine Ecosystems Modeling and Monitoring by Satellites, CLS, Satellite Oceanography Division, 8-10 rue Hermes, 31520 Ramonville, France
[2] Oceanic Fisheries Programme (OFP), Pacific Community (SPC), BPD5, 98848 Noumea, New Caledonia
[3] Current Address: Applied Ecology Centre, University of Canberra, Canberra, ACT, Australia

Predicting skipjack tuna dynamics and effects of climate change using SEAPODYM with fishing and tagging data.

Inna Senina[a] Patrick Lehodey[a] Beatriz Calmettes[a] Simon Nicol[b]
Sylvain Caillot[b] John Hampton[b] Peter Williams[b]

[a]Marine Ecosystems Modeling and Monitoring by Satellites, CLS, Satellite Oceanography Division. 8-10 rue Hermes, 31520 Ramonville, France
[b]Oceanic Fisheries Programme, SPC, BPD5, 98848 Noumea, New Caledonia

Contents

1 Executive Summary

SEAPODYM is a model developed for investigating spatiotemporal dynamics of fish populations under the influence of both fishing and environment. The model is based on advection-diffusion-reaction equations describing dynamic processes (spawning, movement, mortality), which are constrained by environmental data (temperature, currents, primary production and dissolved oxygen concentration) and distributions of mid-trophic (micronektonic tuna forage) functional groups. The model simulates tuna age-structured population dynamics with length and weight relationships obtained from independent studies. Different life stages are considered: larvae, juveniles, immature and mature adults. At larvae and juvenile phases fish drift with currents, later on they become autonomous, i.e., in addition to the currents velocities their movement has additional component linked to their size and the habitat quality. From the pre-defined age at first maturity fish start spawning and their displacements are controlled by a seasonal switch between feeding and spawning habitats, effective outside of the equatorial region where changes in the gradient of day length are marked enough and above a threshold value. The last age class is a "plus class" where all oldest individuals are accumulated. The model takes into account fishing and predicts total catch and size frequencies of catch by fishery when spatially distributed fishing data are available. A Maximum Likelihood Estimation approach is used to estimate model parameters based on fishing data (catch and length frequencies) and conventional release-recapture tagging data. The current paper describes the most recent application of SEAPODYM model to skipjack *Katsuwonus pelamis* population in the Pacific Ocean with INTERIM-NEMO-PISCES (1979-2010) forcing. The optimal model solutions are extended to the Indian ocean and the climate projections are presented for the outputs from three climate models (IPSL, GFDL and NorESM) under the same RCP8.5 IPCC scenario.

1.1 SEAPODYM v3.0

An updated version of SEAPODYM 3.0 was used in the current application to skipjack tuna. The major changes implemented in this version that allowed improvements of the optimized solution for skipjack are:

1. Revision of the spawning habitat with prey and predator functions defined separately (instead of using the prey-predator ratio as in previous version).

2. One additional parameter associated to each functional group of prey can be estimated providing more flexibility in the representation of vertical behavior and access to tuna forage.

3. Implementation of alternative approach to account for fishing mortality and to predict catch without fishing effort, i.e. based on observed catch and model biomass only, which can be particularly useful when reliable fishing effort is not available.

4. Use of geo-statistical methods in integrating observed tag recapture data.

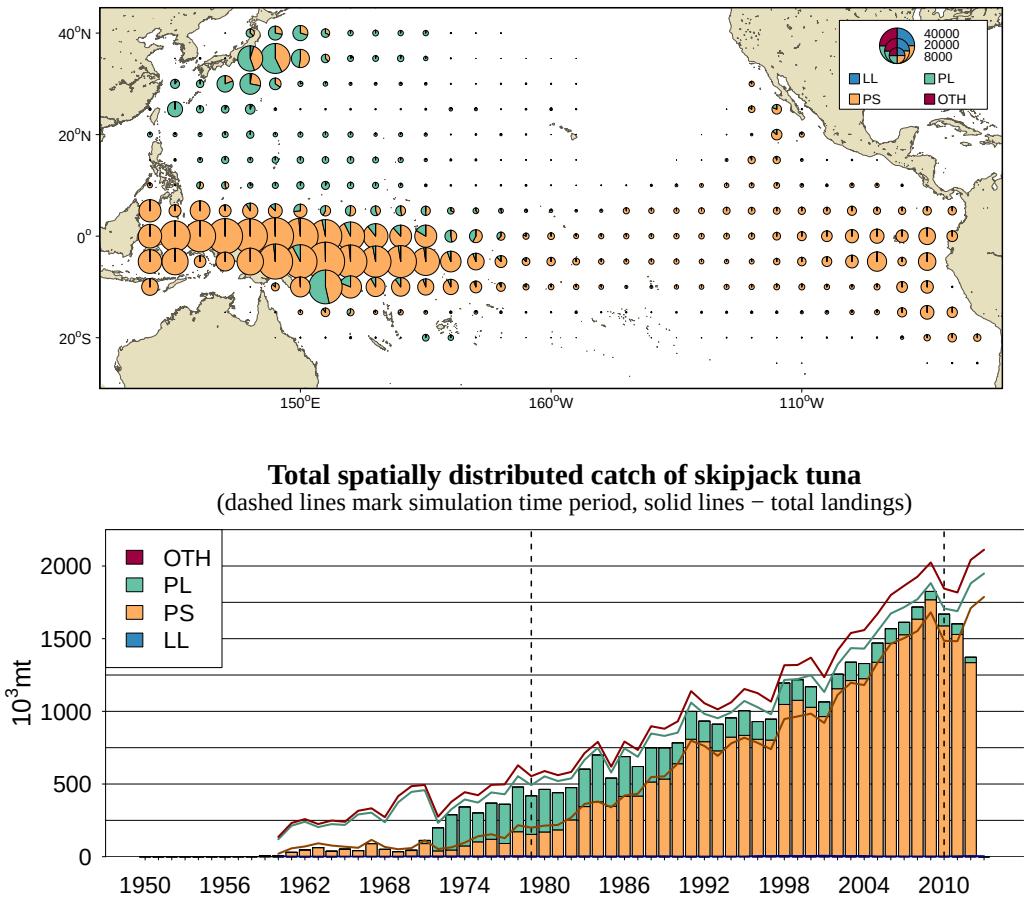

Figure 1: Top panel: total spatially-distributed catch of skipjack population (Pacific-wide) being used in SEAPODYM analyses. Bottom panel: Comparison of total annual catches from spatial fishing dataset and from declared port landings (SPC Year Book, 2012).

1.2 Skipjack tuna fisheries

The industrial fishing fleets targeting skipjack tuna comprise mainly two fishing gears - purse seine and pole-and-line (see [SPC Yearbook 2012]) with the majority of catches coming from purse-seine fleets in WCPO. There are also a few accidental long-line catches of skipjack. Total annual catches by gear being used in the current SEAPODYM analyses are shown on the top panel of the Figure 1. There are some discrepancies between nominal and geo-referenced catches, coming from the coastal domestic fisheries. Unfortunately, these data are unavailable in geo-referenced format, but their absence will unlikely affect the model analysis on the basin scale (see Figure 1, bottom panel).

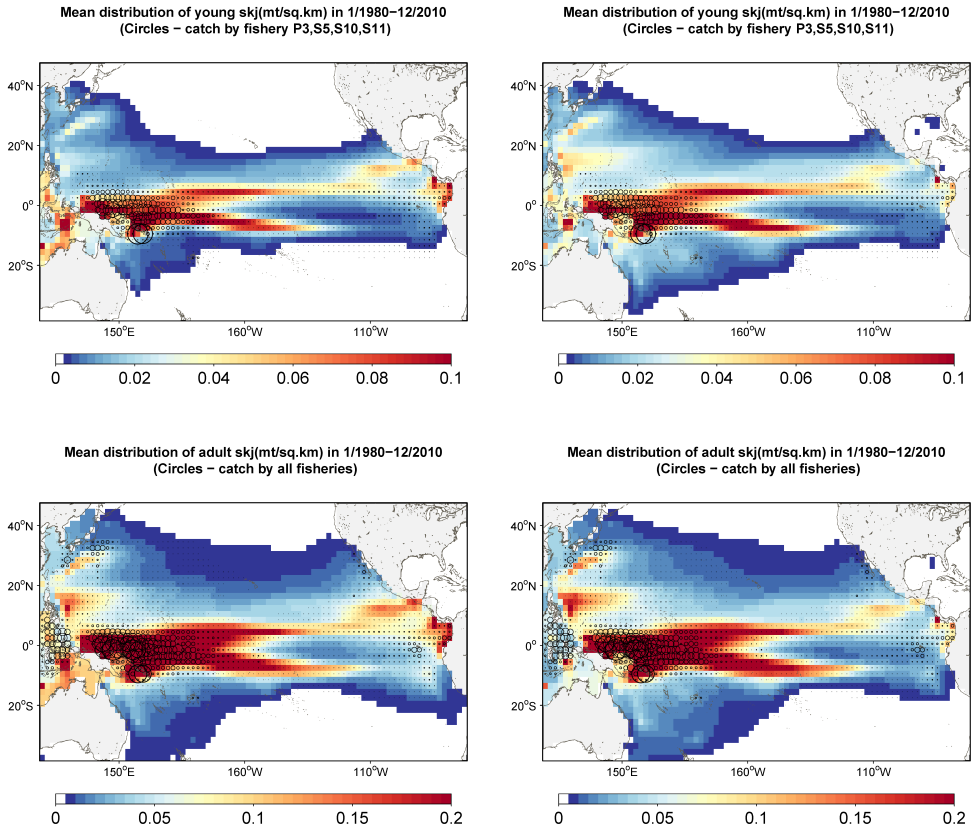

Figure 2: Average spatial distributions of young (left) and adult (right) biomass predicted with E2 (left) and E3 (right) experiments (see text for more details).

1.3 Environmental forcing

The new long-term reference solutions (1979-2010) are developed using a recent hindcast simulation INTERIM-NEMO-PISCES, hereafter INTERIM, prepared by the Institute of Research for the Development (O. Aumont, M. Dessert, T. Gorgues and C. Menkes). This simulation of the historical physical and biogeochemical ocean state is extended with several projections of potential climate change impact (see [Nicol et al, 2014]) based on three climate models: IPSL, GFDL and NorESM under the RCP8.5 IPCC scenario.

1.4 Main results

1. Three parameter estimation experiments are detailed. The third one (E3) is proposed as the new reference solution and provided with a 2° x 30 days for the 1979-2010 period using hindcast INTERIM forcing and optimization with both fishing and tagging data (Figure 2). In comparison to previous reference solution that were obtained with only fisheries data, the new solution exhibits more heterogeneous spatial distributions due to higher advection rates and more variable habitats with high local gradients. As the result the species biomass is concentrated in the favourable habitats with much less "cryptic" biomass elsewhere.

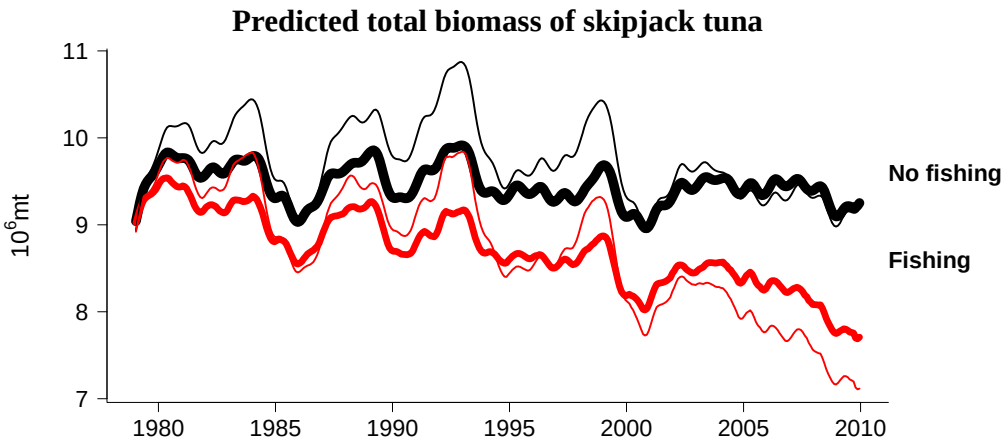

Figure 3: Total skipjack stock Pacific-wide estimated with two different optimization experiments with tagging data (E2 - thin lines and E3 - thick lines, see Table 3 and main text for more details). The black lines show the virgin (without fishing) biomass and the red lines show the biomass of exploited stock.

2. The total biomass is estimated to be 8.1Mt Pacific-wide excluding the Philippine-Indonesia region (120E-70W,20S-45N) and the fishing impact is about 20% of virgin biomass, reaching 25% for adults at the beginning of 2010 (see Figure 3).

3. The use of tagging and fishing data in an optimization experiment with a long INTERIM 2° x 30 days ocean reanalysis allowed estimation of all model parameters, including recruitment, mortality rates, habitat indices parameters and movement rates. Only one parameter (maximal predation mortality) was fixed in the optimization experiments as it is correlated with the number of one-month recruits that is difficult to estimate in the absence of the data on early life stages. The optimal model parameterisation suggests average monthly advection values between 0.7 BL/sec for the 3-month old and 0.1 BL/sec for the 4-year old cohort that are higher than in previous SEAPODYM studies.

4. With the revised definition of spawning habitat functions, the optimization suggested quite strong response of the larvae distribution to both primary production (proxy for the food of larvae) and to the micronekton density (predators of larvae) leading to seasonal favorable "hot spots" for spawning in EPO (April to June with maximum in May), central Pacific (May-August) and in the north-west of East China Sea (spawning habitat is close to 1 in August-October). Some seasonality of spawning index is also predicted in Bismarck Sea, where the larvae densities are high from May to November, while very little spawning occur between December and February.

5. The mean natural mortality rates are estimated between 0.17 and 0.3 mo^{-1} with variability due to environment between 30% for juveniles and 2% for young and adult cohorts.

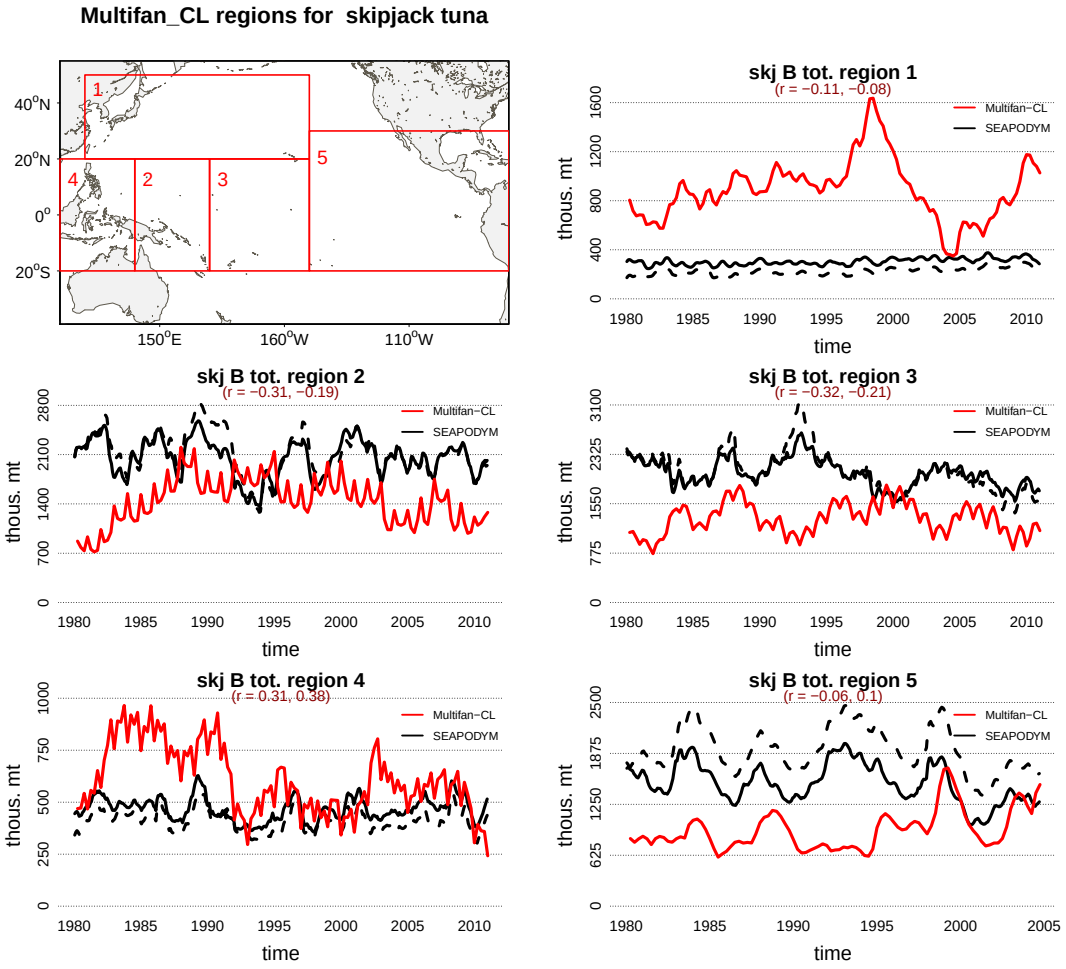

Figure 4: Regional comparison between SEAPODYM (black lines: dashed line - E2, solid line - E3) and Multifan-CL model predictions for total (immature and mature) biomass

6. The purse-seine catches were computed without fishing effort in all optimization experiments. The spatial fit to observed catch was then evaluated using standard method to predict catch (based on fishing effort) after estimating independently (while other parameters kept fixed) the catchability parameters. The fit to the observed catches is good for all equatorial fisheries, however, it deteriorates in the areas with complex current systems such as Kuroshio and Humboldt (Peru coast), where skipjack catches are seasonal. The overall fit to size frequencies samples are generally good.

7. This model configuration and parameterization produced a biomass distribution with a core area associated to the warm waters of the warm pool and the warm Kuroshio currents moving north and the north equatorial counter current moving east. In the eastern Pacific the high densities of skipjack are predicted in the zones of upwelling off the coast of central America and in the area between NECC and California current (see Figure 2).

8. While the total stock estimates in WCPO are very close between SEAPODYM and

Multifan-CL [Rice *et al.*, 2014], i.e. 3.4Mt of adult and about 4Mt of total biomass[1] in 2010, the regional stock estimates differ between the two models by region, especially in the sub-tropical region 1, where MFCL predicts much higher and more variable abundance of skipjack (see Figure 4). On the other hand SEAPODYM predicts higher biomass in the two core tropical regions (2 and 3) known to be the main fishing grounds for skipjack. The EPO estimates is compared to the only available Pacific-wide configuration of MFCL published in [Sibert *et al.*, 2006]. SEAPODYM suggests almost twice larger stock (1.6Mt against 0.8Mt) at the beginning of the simulation and the model predictions approach at the end of MFCL time period reaching about 1.6Mt in both models. It is interesting to note that even though the trends are the opposite, the temporal variability is predicted similarly by both models.

9. Climate change projections with no fishing scenario and three forcing datasets (IPSL, GFDL and NorESM) showed 1) the same long term decreasing trend in the Indian Ocean biomass after the mid-century, with the IPSL forcing leading to the largest decrease, the GFDL to the smallest and the average climate driven reduction of 50%; 2) either no long term decline (NorESM) or a decrease arriving in the mid-century (IPSL) or later after 2080 (GFDL) for Pacific skipjack biomass with clear eastward shift in the biomass distributions in all three simulations (see Figure 5).

10. The main driver of the skipjack biomass decline in the climate change projections is the warming of surface waters affecting the spawning and larvae development. A large portion of the current spawning habitat becomes less and less favorable, especially in the equatorial Pacific warm pool and the eastern equatorial Indian Ocean. IPSL predicts the strongest temperature increase in these regions and consequently the largest decline in larval recruits and then population biomass (Figure 5). Additional simulations conducted with climatological variables confirmed that without an SST trend the stock would maintain and even increase its biomass (without fishing) in the Pacific Ocean. It is worth noting that the species adaptation to warmer spawning temperatures that may mitigate the effects of temperature on the spawning success was not taken into account in the simulations.

1.5 Current and Future Work Plan

1. Climate change projections will be completed and corrected from existing drift in the environmental forcings to provide an envelop of forecast.

2. The operational real-time global (1/4° x 1 week) and regional INDESO (1/12° x 1 day) models will be upgraded with this new reference solution achieved with SEAPODYM 3.0 after downscaling to target resolution and parameterizing the model accordingly.

[1] Figures computed using the catch mask, i.e. extracting the biomass over the grid cells with at least 5% coverage by fishing data.

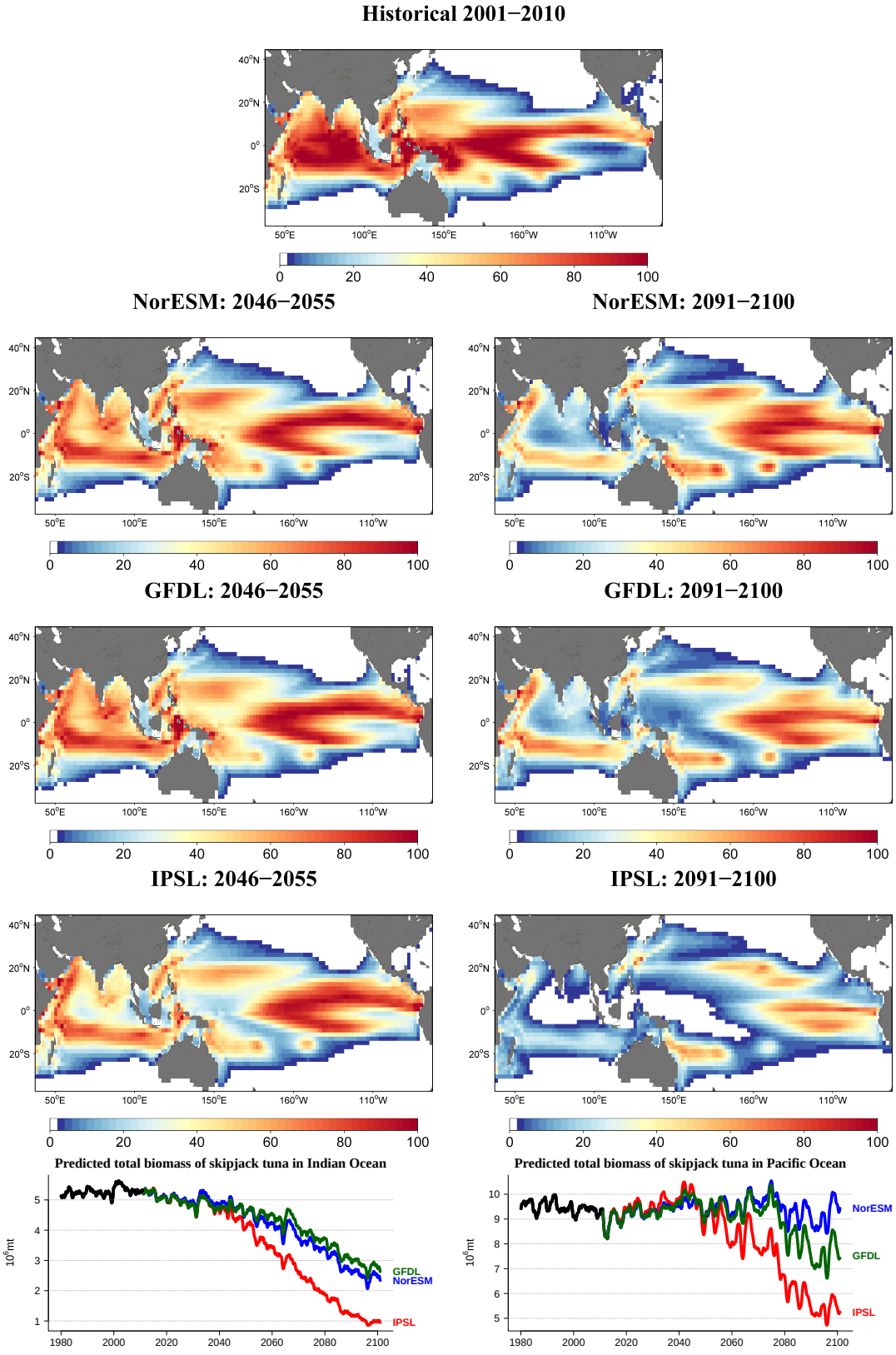

Figure 5: Historical mean (simulation with fishing) and projections of climate change impact (without fishing) on the distribution of skipjack tuna larvae for the mid-century using atmospheric outputs from 3 different Earth Models under IPCC RCP8.5 scenario to drive the coupled physical-biogeochemical NEMO-PISCES model and then SEAPODYM.

3. Improvement of micronekton model (functional groups of prey for tuna) is continuing with acoustic data used for parameter optimization.

4. SEAPODYM documentation and website need to be updated.

1.6 Acknowledgments

We thank Kurt Schaefer and Dan Fuller from IATTC for sharing the conventional tagging dataset that was used in the validation study. The continued development and application of the SEAPODYM model to the work of the WCPFC Scientific Committee is facilitated through Project 62. The project affiliates the independently funded work on SEAPODYM into the SCs work programme. It is conducted in collaboration with the Oceanic Fisheries Programme (OFP) of the Secretariat of the Pacific Community. Project 62 is currently supported by Collecte Localisation Satellites, a Climate Change and tuna project coordinated by the Oceanic Fisheries Programme at SPC and one project funded by the Government of Indonesia and the Agence Francaise de Developpement. The Inter American Tropical Tuna Commission has provided access to non-public domain data for the purposes of progressing the work programme of the WCPFC-SC.

2 Introduction

This paper presents the most recent application of SEAPODYM to Pacific skipjack tuna population (*Katsuwonus pelamis*) in the Pacific Ocean. It is based on the last SEAPODYM version 3.0 that includes several major changes related to the habitat indices estimation and the use of tagging and fishing data. Compared to previous work [Lehodey *et al.*, 2009], the model optimization was done with the full set of data, including fishing and conventional release-recapture tagging data. This study relies on the data from PTTP tagging experiment conducted by SPC, namely the data between May 2008 and December 2010. The integration of tagging data allowed better estimation of habitat indices parameters and movement rates. The estimation of all model parameters was performed in the optimization experiments for the whole Pacific Ocean and 30-years long historical simulation (1979-2010). Such long term optimization experiments are essential to estimate the parameters of the larvae-stock recruitment relationship. The fishing data and fisheries definition have been carefully revised before running this new model configuration. Once optimal parameterization is achieved, the model is used to estimate the fishing and environmental impact and then to run the climate change projections. The climate simulations were produced with environmental variables provided by the same coupled model, without fishing impact, and using three different atmospheric forcings: IPSL, GFDL and NorESM under the same RCP8.5 IPCC scenario. The objective is to increase the number of projections to provide an ensemble of simulations and thus to measure the uncertainty in the future trend of the skipjack tuna population.

3 Background

3.1 Biology

Skipjack tuna is known as a rapidly growing (mature in 10 months) species with rather short life span (5 years) and small size (40-60cm FL) in comparison to other tuna species. It is the most abundant tuna species in the Pacific Ocean with the most significant contribution to the total tuna catches. Skipjack inhabits surface (epi-pelagic) layers and prefers warm waters of the tropics and warm current systems (Kuroshio, Humboldt) in sub-tropical areas. Adult skipjack can be found in water masses with wider temperature range, however the total distribution is limited to the 20°C surface isotherm. From the revision of all published data undertaken by [Boyce *et al.*, 2008] the optimal temperature for adult skipjack ranges between 19°C and 26°C. The skipjack larvae are abundant in waters above 26°C but some can be found in temperatures down to 22°C [Boehlert and Mundy, 1994]. Skipack is sensitive to the oxygen, which explains why this species vertical distribution is restricted to the upper layer. The species prefers waters with dissolved oxygen levels above 5 mg/l (3.8 ml/l) while the levels of oxygen being 2.45 mg/l and 2.83 mg/l are lethal for 50cm and 75cm individuals correspondingly [Brill, 1994]. From tagging data and model analysis it is known that skipjack tuna is highly mobile animal [Sibert *et al.*, 1999] and that the population movement rates are influenced by the oceanographic environment [Lehodey *et al.*, 1997].

3.2 Fisheries

The industrial fishing fleets targeting skipjack comprise mainly two fishing gears - purse-seine and pole-and-line. There are some incidental skipjack catches by long-line fleets targeting bigeye and yellowfin, but they account for less than 0.1% of total skipjack catches Pacific-wide [SPC Yearbook 2012]. In addition there are variety of other gears (gillnet, hook and line, ring net) exploiting skipjack population in the Philippines and Indonesia and in many of the Pacific Islands.

The catches of skipjack in the Pacific ocean increased steadily since 1970 with the rapid increase of purse-seine catches in the late eighties and consequent reduction of pole-and-line catches (see Figure 1). The pole-and-line gear is represented mostly by the Japanese fleets operating all year around in the tropical WCPO and seasonally in Kuroshio area (see Figure 28). In addition there are small domestic pole-and-line fisheries in PNG and Solomon Islands in WCPO and baitboat fishery in EPO with boats from Equador, Mexico and United States (Figure 28).

Purse-seine fleets are targeting skipjack around FADs, in associations with other floating objects, whale sharks (WCPO) and dolphin schools (EPO). The catch by purse-seine gear comprise about 85% of total skipjack catches

During the period of model analysis (1979-2010) the total annual catches of skipjack peaked in 2009 when the tropical purse-seine fleets caught 1.7Mt with largest portion coming from FAD and LOG associated fisheries. However, followed by restrictive measures that were put in place by WCPFC after the 5th regular meeting in 2008 in order to reduce bigeye mortality by 30% [WCPFC, 2008], this high catch might be due to over-reporting of skipjack and under-reporting of yellowfin and bigeye in log-books [Rice *et al.*, 2014].

4 Data

4.1 Fishing data

The industrial fishing fleets targeting skipjack comprise mainly two fishing gears - purse seine and pole-and-line [SPC Yearbook 2012], the catches of skipjack by long-line gear are incidental selecting only large adult skipjack. Total annual catches by gear being used in the current SEAPODYM analyses are shown on Figure 28. Skipjack tuna geo-referenced fishing data are provided by SPC and IATTC (Figure 1). Each fishery in SEAPODYM is defined by a single selectivity function and a catchability coefficient that is allowed to increase/decrease linearly with time. Removing the fisherman-driven causes of changes in catchability, such as changes of target species or the fishing strategy, we assume that the remaining variability in catchability is driven by the spatial distribution associated with the environmental variability and fish movements, which are explicitly described by the model. Therefore it is critical to have a definition of homogeneous fisheries in terms of constant in space and time catchability and selectivity coefficients. The definition of fisheries for Pacific skipjack tuna, which is assumed to satisfy to such criterion is provided in Table 1.

It is also important to have the complete geo-referenced dataset that corresponds to the total landings in terms of total annual removal from the stock in order to correctly take into account the mortality due to fishing (see Figure 1. Small discrepancies exist between

WCPO purse-seine catch data during the last two years of simulation period representing less than 5% of the PS yearly catches. Larger differences exist for pole-and-line and for an ensemble of artisanal fisheries (referred as OTHER gears).

Size frequency data provided by SPC (Pacific-wide long-line data and purse-seine in WCPO area), have variable resolutions ranging from 1° x 1° to 10° x 20°. In the EPO the size data are provided for purse-seine fleets over IATTC sampling regions (see http://www.iattc.org/Meetings2010/PDF/Aug/SAC-01-11-Port-sampling-program.pdf).

4.2 Tagging data

A considerable effort has been deployed in the Pacific Ocean for tagging tuna with a conventional approach (Fig. 6). The first tagging campaigns started in the sixties in EPO and late seventies in WCPO (see Figure 7), with the majority of the releases made in the tropical Pacific Ocean. In particular, SPC has conducted several large tagging experiments, releasing several hundred thousand of tagged fish since the 1980s in the western and central Pacific region, essentially skipjack and yellowfin. The latest tagging experiments conducted by SPC since 2008 has deployed 199,075 conventional tags on skipjack in the western central equatorial region (35,543 have been recaptured so far). IATTC and the Japanese Fisheries Agency have been also very active in tuna tagging, in the eastern and north-west Pacific respectively, providing key information to investigate the dynamics of the stocks at the scale of the whole basin and exploring the interactions between these different oceanic regions, particularly under the influence of ENSO.

Conventional tagging data are integrated into the optimization method in SEAPODYM to improve the estimates of habitat and movement parameters. Only the recapture data are used in the model (see the Method section). Due to better quality of the recapture positions that could be checked with VMS data, only the recent release-recapture data starting in 2008 were used in the optimization experiments and the rest of the dataset was used to validate the model solutions. The important reason to choosing the control sub-set is the reduction of the computational cost, that depends on the number of tagged cohorts to be numerically resolved. This tagging data sub-set temporal coverage and the distribution in terms of mean length and time at liberty is illustrated on the Figure 7.

5 The model configuration

5.1 Physical and biological forcing

SEAPODYM uses spatially explicit estimates of ocean and biological properties such as temperature, current speed, oxygen, phytoplankton concentration and euphotic depth from physical and biogeochemical ocean models to constrain tuna population dynamics. The outputs of SEAPODYM are therefore strongly dependent on the quality of its forcing.

The physical variables (temperature and currents) are outputs of ocean circulation models, either from hindcast simulations or reanalyses. They both provide the same outputs but in the first case the ocean model is forced by atmospheric variables (eg. surface winds) only. In reanalyses, the simulation also includes observations of oceanic variables (e.g. Argo profilers, satellite altimetry) that are assimilated in the model to

correct the model and produce more realistic circulation patterns, especially at mesoscale resolution.

The biogeochemical variables (primary production, dissolved oxygen concentration and euphotic depth) can be obtained from a biogeochemical model that is coupled to the physical model or from satellite ocean color sensors from which chlorophyll-a, euphotic depth and vertically-integrated primary production are estimated. However, in that case the dissolved oxygen concentration is not available and needs to be replaced by a climatology (i.e., monthly average based on all available observations). All physical reanalyses are used with biogeochemical variables derived from satellite ocean color data.

All forcing variables are interpolated on the same regular grid and same time step prior to the use in SEAPODYM simulations. The mask is based on physical data availability at the levels of depth. The euphotic depth is used for averaging the physical data over three vertical layers: (1) Epipelagic layer, between the surface and 1.5 the euphotic depth (2) mesopelagic layer, between 1.5 and 4.5 the euphotic depth and (3) Bathypelagic layer, between 4.5 and 1.5 the euphotic level.

The configuration of current SEAPODYM application is summarized in Table 2. Each configuration refers to pre-processed dataset including physical, biochemical and biological variables listed in Table 2.

5.1.1 INTERIM

The INTERIM configuration (1979-2010) includes both physical and biogeochemical forcing provided by IRD: NEMO ocean model was coupled to the biogeochemical model PISCES (Pelagic Interaction Scheme for Carbon and Ecosystem Studies, Aumont and Bopp, 2006) at a coarse horizontal resolution of 2° (ORCA2 grid with a refined resolution of 0.5° in the equatorial band), see [Nicol et al, 2014]. It is forced by the ERA40-INTERIM atmospheric reanalysis (atmospheric temperature, zonal and meridional wind speeds, radiative heat fluxes, relative humidity, and precipitation) which has been corrected using satellite data (Dussin et al., 2013). Salinity, temperature and biogeochemical tracer concentrations (nitrate, phosphate, iron, silicate, alkalinity, dissolved oxygen and dissolved organic and inorganic carbon) were initialized from the World Ocean Atlas climatology (WOA09, Garcia et al., 2009), and model climatologies for iron and dissolved organic carbon. This simulation was produced for SPC by the French Institute for Research and Development [Nicol et al, 2014].

5.1.2 Climate Change Projections

Coupling ocean biogeochemistry with atmosphere-ocean models is expensive as is the optimization of SEAPODYM to numerous physical forcings of future climate. A pragmatic approach is developed (Nicol et al 2014) to produce an ensemble of simulation under IPCC scenarios based on a single physical forcing of the historical period (i.e., the INTERIM configuration above). SEAPODYM can then be optimized to this forcing which can then be used as the parameterizations for subsequent forecasts using each climate model. The NEMO ocean model (version 3.5) is forced with atmospheric trends extracted from coupled climate models for the RCP8.5 scenario [IPCC 2014] and coupled to the biogeochemical model PISCES (Pelagic Interaction Scheme for Carbon and Ecosystem Studies, Aumont and Bopp, 2006) following the same configuration used in INTERIM.

With this method, the dynamic and biogeochemical state of the ocean for the 21st Century is simulated using atmospheric variables predicted from three Earth climate models involved in the Coupled Model Intercomparison Project Phase 5 (CMIP5). They are the IPSL, GFDL, and NorESM models. They all generate internal interannual variability similar to the El Niño Southern Oscillation (ENSO) cycles in their simulation [Bellenger et al., 2013, Table 2].

5.2 Static model parameters

The model is numerically solved on a 2° regular grid and monthly time step. The age is discretized between 0 and $\mathsf{age}_{max} = 4$ (yr) into monthly cohorts resulting in 37 cohorts for skipjack, so the first three years are split into 36 monthly age classes and the last year individuals are aggregated into a single cohort.

Some parameters cannot be estimated in SEAPODYM and should be configured for each model run. These parameters are age-length and age-weight relationships. For the current run they were derived from the 2014 MULTIFAN-CL estimate [Rice *et al.*, 2014].

One more model parameter, the maximal predation mortality at age 0, is set to constant in the current optimization experiments. In the absence of direct observations at early life stages, which could be assimilated within parameter estimation procedure, the predation mortality parameter is highly correlated with the reproduction rate as they both act linearly on the local densities of the first cohort with only one time step delay.

Also, from previous optimization runs it was found that seasonal spawning migrations (as they are currently implemented in SEAPODYM) are estimated to be not effective for skipjack, so this functionality was switched off in the optimization experiments, which allowed some reduction of computational cost given high demands due to the use of tagging data. The species is thus assumed to be opportunistic spawner with a spawning success proportional to the spawning habitat index.

5.3 Initial conditions

The INTERIM forcing (see Table 2) was provided for the time period 1/1979-12/2010. The initial conditions for 1979 were obtained using the the SEAPODYM-NCEP 2° - 2-month age structure model (see [Lehodey et al, 2014]). In the optimization runs the first 4 years were however skipped in order to forget the initial conditions, thus only the data during the time period 1983-2010 were used to estimate the control parameters.

5.4 Optimization

In the current optimization experiments, the resolution used to compute the likelihood term for the tagging data was 6° in latitude and longitude, and a 3-month time step. However, the validation of the optimization results was then done on the model spatio-temporal resolution, i.e. 2° and 1 month.

The new catch removal method to account for the fishing mortality independently of fishing effort and catchability was implemented and used in this optimization study. It consists in removal of the total catch at age directly from the biomass simultaneously with the natural mortality and transport processes described by the model ADREs. Local

predicted catch is exactly the observed catch if the local predicted biomass at age is sufficient to sustain this level of catch. If it is not the case the predicted catch will be the total local available biomass (by age). Obviously, the use of such predictions in the likelihood allows observability of model parameters only in the grid cells where the predicted biomass is lower than the observed catch. It should be noted that the catch removal method cannot be used alone because of its obvious tendency to overestimate the biomass in order to fit the highest local catches. To counterbalance this tendency, a prior information to constrain the average stock value was added to the likelihood function with the objective to find the minimal stock given the spatial distribution that supports all local catch levels. This value was set to 8,000,000 mt Pacific wide (120°E - 70°W, 20°S - 45°N). Note, this value is chosen for it is the lowest possible stock sustaining the current fishing pressure, i.e. corresponding to the descrepancies between total observed and predicted catch smaller than 20% of the total catch levels.

In this analysis, the definition of spawning habitat index, and hence the spawning success in the model, was revised to estimate independently the effects of food availability and larvae predators density. They were previously combined using a ratio between densities of food and predators. The new definition implies the use of three additional parameters (see Table 4, section Reproduction).

Following the work done for bigeye model with tagging data ([Lehodey et al, 2014]), six (by number of micronekton groups) new parameters were added to define the distribution of the feeding habitat and hence to provide additional flexibility in its estimation. These parameters assign a weight to each micronekton group used to compute the feeding habitat index, based on their biomass and accessibility (see parameters eFn in the Table 4).

The negative log-likelihood to be minimized is the sum of three main components that include the catch data, the length-frequencies data and the tagging data. Note that for the fisheries, for which the catch removal method is used we choose the normal likelihood profile because the errors are proportional to the modelled biomass and hence can be assumed normally distributed. When the catch of a fishery is predicted using the fishing effort, then the Poisson likelihood is used as in [Senina *et al.*, 2008]. The robust likelihood function formulation proposed by [Hampton and Fournier, 2001] is used for the length frequencies data.

In order to test the impact of the use of each observational dataset and of the likelihood function formulation, we performed a set of optimization experiments. First, we were interested in the major change that is brought to the model predictions by the use of tagging data. However, we must have been sure that the change was not attributed to the new catch removal method or to the functional forms of likelihoods to account for the errors between predicted and observed catches. That is why several experiments were done to explore all options. Although we will discuss the outcomes of all optimization experiments in this paper we will present and compare the solutions of only three alternative experiments, which demonstrate the importance of including different types of observations and allow us to separate out the role of tagging data in predicting the dynamics of tuna species. In the experiment E1 we used only fishing data (catch and length frequencies), and only the pole-and-line fisheries (both tropical and sub-tropical) were predicted based on fishing effort, the purse-seiners activity was included using the catch removal mehthod. The pole-and-line fisheries were selected since they target primarily skipjack

and the fishing effort data is believed to be homogeneous, correctly geo-referenced and well reported. Therefore, in the absence of tagging data, a strong weight is put on this fishery to estimate the skipjack habitats and movements parameters. In the experiment E2 both fishing and tagging data were included in the likelihood and all catch data was predicted using the catch removal method, even for pole-and-line fisheries. The experiment E3 was configured the same way as E2, but with the pole-and-line catches computed as in E1. Note that long-line fisheries were not included in all three experiments due to scarcity of the well reported data for skipjack.

6 Results

6.1 Parameter estimates

Estimated model parameters driving population dynamics are listed in the Table 4. The fishing parameters are not shown. The optimal spawning temperature was estimated between 28°C and 29°C in three experiments: 28.52°C, 28.96°C and 28.5°C in E1, E2 and E3 respectively. The standard error is the smallest in E2 (1.37) and the largest in E1 (2.5). The resulting functions determining the thermal function of the spawning habitat can be seen also on the Figure 6. The highest optimal temperature for the spawning with the smallest tolerance interval results in more patchy and more restricted to the tropics spawning habitat. This result can be attributed to the use of tagging data, which delineate a highly concentrated distribution of skipjack in the tropical waters and much smaller densities in the transition zones. Skipjack are known to have spawning activity peaking between 26°C and 30°C [Schaefer, 2001], and an overall species distribution identified from all historical occurrences between 17°C and 30°C [Sund et al., 1981].

The optimization with the tagging data and without the fishing effort in the catch prediction (E2) suggested the strongest response of the larvae distribution to both primary production (proxy for the food of larvae) and to the micronekton (predators of larvae) density (see Figure 6, dashed line). This leads to the seasonal favorable "hot spots" for spawning in the EPO (April to June with maximum in May), central Pacific (May-August) and in the north-west of East China Sea (spawning habitat is close its maximum value in August-October). Some seasonality of the spawning index is also predicted in Bismarck Sea, where the larvae densities are high from May to November, while very little spawning occurs between December and February. We note also that with regards to the predators density the E3 solution provides the weakest response. It seems that fitting to the pole-and-line catches in the sub-tropical areas the function minimizer tends to reduce the impact of this key variable in order to increase the biomass of skipjack in the sub-tropical waters all year round. The latter means that the model capacity to predict migrations towards these areas is still limited, the reasons being either the coarse resolution of the physical forcing or/and a wrong habitat index formulation, which does not provide the correct gradient field for timely seasonal migrations.

In all three experiments the stock recruitment relationship parameters were released. The estimated functional forms of this relationship (between the spawning biomass and the amount of larvae survived after one month) are shown on Figure 6. The strongest relationship providing the non-linear response over the whole range of model densities of adults, is estimated in the experiment E2. The solution E1 predicts the impact of adult

density on larvae abundance only for small interval of values, and E2 is placed in between the two other experiments. The stock-recruitment parameter is estimated at its upper boundary in E1, which means that the E1 solution for the larvae became insensitive to the adult distribution and extending the boundary to higher values allowing the parameter to reach the zero-gradient point would not change this result.

The optimal temperature for feeding habitat of adults was estimated and gives a thermal habitat decreasing with size/age from 28.7°C to 26.2°C, which are the same in E2 and E3, but lower (between 27.7°C and 25.8°C) for E1. This result is attributed as well to the use of tagging data in the likelihood, which makes E2 and E3 different from E1. The current temperature estimate implies the accessibility of skipjack only to the epipelagic layer. This is also seen from the estimates of MTL groups contributions to the habitat (Table 4), which are estimated non-zero only for resident epipelagic and highly migrant bathypelagic forage (inhabits pelagic layer at night).

The values of the oxygen function parameters were estimated with minor differences in all three experiments - 3.5, 3.65 and 3.64 ml/l in E1, E2 and E3 respectively. These parameters are usually well estimated for skipjack, which has low tolerance to poorely oxygenated waters.

The difference in the estimates of movement parameters in the experiment E1 and E2-E3 is well pronounced. The highest diffusion rates and lowest advection rates are estimated in E1. This leads to predicting the non-zero densities of skipjack outside of its preferred habitat (see Figure 12). It is interesting that in the experiment E3 there are less movement parameters estimated at their boundaries, which may indicate that pole-and-line fisheries effort and catch data were indeed complementary to the tagging data and helped to constrain movements where the tagging data are less present, e.g. in sub-tropical regions.

The estimated theoretical mortality curves are very close between E2 and E3, providing the mean natural mortality rates enclosed within the interval 0.15 - 0.25 mo-1. SEAPODYM values are generally higher than those of Multifan-CL [Rice *et al.*, 2014] (see Figure 6), which estimates skipjack mortalities varying between 0.09 - 0.22 mo-1. However, the mortality profile of E1 is very different, with low mortalities for young cohorts and rapidly increasing mortality rates after the age at maturity (about 1 year). Such estimates mean that a very few old fish is predicted by the model with E1 parameters, namely there is only 5% of skipjack recruits left after the age of two years. This result may be explained by achieving the stronger variability of the population distributions due to the environment-stipulated recruitment rather than due to migrations. Note that the impact of tagging data in this case will be indirect as the mortality parameters are not observed through the recapture data. Such hypethesis should be verified with more optimization experiments by leaving out the possibility of the critical role of fixed $\bar{m}_p$ parameter and of the initial guess values. The variability of mortality with habitat index is excluded by the function minimizer. This was previously observed in earlier experiments [Senina *et al.*, 2008, Lehodey *et al.*, 2009] that this parameter has low sensitivity to skipjack data and that the food requirement index works better, however the later option was not switched on in the current experiments to avoid excessive computations.

6.2 Validation

Although the parameter estimation was performed with the 2008-2010 tagging data subset, the validation of the fit to the tagging data was done using the whole dataset (see Figure 6 and 7). The spatial fits to the distributions of recaptured tags are compared between E1 and E2/E3 (the differences are not detectable on the color map) on Figure 9. It is clearly seen that the full likelihood experiments provide the better fit to the tagging data. The longitudinal extension of tag recaptures is much better reproduced in E2 and E3. The movements towards higher latitudes are still mediated by diffusion as smaller concentrations of skipjack recaptures are predicted east of Japan coast while the distribution with non-zero values is predicted in the gyre, where skipjack habitat is unfavorable. The longitudinal and latitudinal profiles of predicted vs observed tag recaptures are shown on Figure 10. There are still some significant discrepancies between the recaptures east of 160E, which are located south of equator. The same experiments with another forcing dataset, providing better representation of currents fields in this zone (e.g. derived from ARGO data, see [Lehodey et al, 2014]) should be used in order to test the impact of the physical forcing (see [Senina *et al.*, 2015]) on the fit to the tagging data and the parameter estimates. The three scores of the spatial fit to the recaptures data - coefficient of determination (Pearson R-squared coefficient), standard deviation ratio (the ratio between standard deviations of model predictions and those of data) and the normalized mean squared error, are also shown on the Taylor diagram (Figure 11, blue symbols). The scores for E2 and E3 are very close being (0.57, 0.59, 0.66) and (0.56, 0.6, 0.67) for E2 and E3 correspondingly and (0.55, 0.27, 0.71) for E1. The score that gets the most deteriorated in E1 with respect to the experiments E2 and E3 (with tagging data) is the relative variability of model predictions. The best value of this score is 1, so the value 0.27 in E1 shows that this solution has much weaker variability in both space and time due to higher diffusion and lower advection rates.

The spatial fit to observed catch predicted with the fishing effort for all fisheries was tested after the catchabilities were estimated (such experiments was conducted with all other parameters being fixed at their optimal values). The scores of this fit are shown on the Taylor diagram (Figure 11, black symbols). Of course, the best validation scores belong to the E1 solution, which was obtained by fitting to the catch data. However, it should be noted that the quality of the fit is determined by the purse-seine fisheries, for which the catches were not predicted with the fishing effort in all experiments. Thus, the score (0.76,0.61,0.5) is fairly good, except for the variability, which is significantly weaker than observed. The scores of E2 and E3 in terms of the fit to the catch data are also good, especially those of E3 (0.71,0.9,0.55) that is close to the E1 in terms of correlation and error, but much better in terms of modelled variability. This is an additional argument to select this solution as the best one.

The fits for the catch data predicted independently of the fishing effort are also compared in order to evaluate how well the model biomass sustains the local levels of catches. Not surprisingly, the best score is demonstrated by the solution E2 (the error 0.18) and the worst is obtained for E1 (0.25). Thua, the most discrepancies are coming from the warm-pool area, where the E2 provides the highest concentrations of skipjack. However, the E1 solution is better than E2 in the sub-tropical areas (not shown), where E2 underestimates skipjack biomass. The latter is corrected in E3 (the error 0.2) due to the fact

that Japanese pole-and-line E/C data were used to constrain the parameter estimation.

6.3 Stock structure and size

Given the stock likelihood term that forces the model to find the minimal stock to sustain catches, the temporal average of the total stock is nearly the same in E1 (7995Mt), E2 (8122Mt) and E3 (8076Mt). Although it may not be so evident from the parameter estimates or from the validation, but the predicted biomass distributions change drastically with the use of tagging data (see the Figure 12). The parameterization of E1 provides very smooth (due to high diffusion rates) distribution with lots of "cryptic" unobserved biomass. The core area associated to the warm waters of the warm pool where the skipjack catches are highest (Figure 12) is characterized by much lower densities of skipjack in E1 than in E2 or E3, see also the regional proportions of skipjack biomass in the Table 5. Based on the parameter estimates and on the validation scores, we will leave the parameterization of E1 out and will now discuss only the results of E2 and E3 experiments.

The skipack stock predicted by the experiments with tagging data is mostly distributed in the warmpool in the tropical area, and warm Kurishio currents moving north and the north equatorial counter current moving east. In the eastern Pacific the high densities of skipjack are predicted in the zones of upwelling off the coast of central America and in the area between NECC and California current (see Figure 12). Both distributions of young and adult tuna are highly concentrated in the existing fishing grounds. There are moderate biomass levels of adults west of Phillipines. The solution E3 predicts lower biomass in the EPO area but more abundant sub-stocks in the sub-tropics.

The overall estimates of reproduction and mortality parameters results in the following composition of skipjack population in terms of total weight by life stage: about 0.1% and 0.2% of juveniles, 21% and 26% of young and 79% and 74% of adult biomass in the solutions E2 and E3 respectively. As seen also from the biomass distribution by age (Figure 13) the skipjack population is a bit younger in E3 with the mean age around 12 months in both parameterizations, but the larger standard deviation and hence more spawning potential in E2. The predicted total stock of skipjack fluctuates between 7 and 10Mt with the maximum in the beginning of the time series and minimum in 2009, but significantly higher variability in E2 (see Figure 3). Note, that these figures were calculated excluding the area west of 120W, i.e. the Philippine-Indonesia regions for which the coarse resolution and lack of data produces high uncertainty. These levels of population abundance correspond to the 5.7-7.5Mt of the total exploitable stock (calculated based on the average selectivity by all gears) during the period 1980-2010 (Figure 14).

While the total stock estimates in WCPO are very close between SEAPODYM and Multifan-CL [Rice *et al.*, 2014], i.e. 3.4Mt of adult and about 4Mt of total biomass in 2010, the regional stock estimates differ between two models, especially in the sub-tropical region 1, where MFCL predicts much higher and more variable abundance of skipjack (see Figure 4). On the other hand SEAPODYM predicts higher biomass in the two core tropical regions (2 and 3) known to be the main fishing grounds for skipjack. Note that in all regions the total predicted biomass in E3 is closer to predictions of Multifan-CL. The EPO estimates are compared to the only available configuration of MFCL published in [Sibert *et al.*, 2006]. SEAPODYM suggest almost twice larger stock (1.6Mt against

0.8Mt) at the beginning of the simulation and the model predictions approach at the end of MFCL time period (2000-2005) reaching about 1.2Mt by both models (solution E3 in SEAPODYM). It is interesting to note that even though the trends are the opposite for EPO, the temporal variability is predicted similarly by both models.

6.4 Fishing impact

The overall fishing impact at the basin scale is predicted to be above 15% for E3 and above 20% for E2. The E2 solution shows the strongest impact of fishing (25% reduction of adult biomass and 10% reduction of young stock at the end of 2010) due to the highest concentrations of skipjack stock within the fishing grounds but also due to the very low biomass estimated in the sub-tropical regions. The fishing impact in E3 is more moderate (20% reduction of adults and 5% reduction of youngs) due to higher biomass levels in the sub-tropics. The spatial maps of fishing impact (Figure 20) show that locally the adult biomass reduction can exceed 50% in the WCPO (PNG area) and 30% in the EPO (upwelling zone near Peru). This impact has certainly increased since 2010, with an annual skipjack catch estimated to almost 2 Mt in 2014 [Williams and Terawasi, 2014].

6.5 Impact of environmental variability

The impact of interannual variability associated to the El Niño Southern oscillation (ENSO) on the distribution of skipjack in the Pacific Ocean has been demonstrated from catch and tagging data (Lehodey et al. 1997). ENSO is an oscillation between a warm (El Niño) and cold (La Niña) state, that evolves under the influence of the dynamic interaction between atmosphere and ocean, with an irregular frequency between 2-7 years. The changes in the trade winds lead to zonal (east-west) extensions/contractions of the warm pool are reflected by the Southern Oscillation Index (SOI), calculated from the difference in sea level pressure between Tahiti and Darwin (Figure 23). A strong negative index indicates an El Niño while a positive index reveals a La Niña event. Following a long sequence dominated by neutral or la Niña events, a powerful El Niño event developed from the end of 2014 with a maximum intensity in 2015.

The skipjack INTERIM simulation predicts interannual variability with sequences of contraction/extension of the species habitat showing the highest densities, for instance like during the strong El Niño event of 1997-98 followed by La Niña in 1998-99 (Figure 23). During such powerful El Niño events, the favorable spawning habitat of skipjack extends all along the equatorial region. If a La Niña event follows a few months later, the skipjack biomass with exceptional recruitment is pushed westward leading to high concentration and catch in the PNG /Solomon region (Figure 24). This mechanism explain a strong relationship between the climate index SOI and the time series of larvae recruits or the total biomass 8 months later, ie the time of development needed between spawning and recruitment peak in the fishery. Then, the combination of either El Niño or La Niña events during multi-year periods, possibly in correlation with the Pacific Decadal Oscillation (PDO), can lead to multi-year regimes of high and low productivity in the tuna populations from which high amount of catch are removed by fisheries.

The INTERIM simulation stopped at the end of 2010 and did not allow investigation of the impact of the recent El Niño event. However, the operational model implemented

for the INDESO project provides a view of the change in the distribution (see the current session's review paper by Nicol and co-authors).

6.6 Climate change projections

The Pacific INTERIM optimization was used to investigate the climate change impact (without fishing) over the 21st Century using three different projections achieved with the same RCP8.5 IPCC scenario (business as usual) but with atmospheric variables predicted from three Earth climate models: IPSL, GFDL, and NorESM. The model was run at global scale allowing to test if the parameterization achieved in the Pacific remains reasonably valid in the Indian Ocean. It was shown from previous analysis [Senina *et al.*, 2015] that the INTERIM configuration was not satisfying for the Atlantic basin as it was not properly predicting the primary production.

Until the mid-century, the overall distribution of skipjack does not show strong changes compared to the predicted distribution of the last decade, both in the Pacific and Indian Ocean (Figure 25). While still preliminary, the analysis of skipjack fisheries in the Indian Ocean indicates a good match with the seasonal distribution of purse seine fisheries in the west. In the east, the model predicts large concentration of skipjack in the equatorial region that is likely overestimated given our knowledge based on fisheries data. This may be due to an overestimation by the INTERIM simulation of the primary productivity in this region as suggested from a comparison with satellite derived primary production. In the Pacific Ocean, the three different forcings give also similar average distributions until the mid-century and close to the average present distribution. After that period however, the three runs diverge. The IPSL projection shows the strongest decrease in adult biomass in the equatorial region and particularly the warm pool. A moderate decrease occurs in the warmpool with the two other runs. The western central tropical 15°N-20°N latitudinal band become more favourable, with a most pronounced change in the GFDL projection.

As a result of these spatial redistributions and dynamics, the total biomass of Pacific skipjack shows a strong decline after 2040 with the IPSL forcing (Figure 26), with a 50% reduction at the end of the Century (without fishing). The decrease is less marked with the GFDL run (25%) and starts later, after 2070. For the third one (NorESM) there is no decrease, the increasing biomass in the tropics compensating the decrease in the equatorial warm pool.

It is worth noting that the model responses in the Indian Ocean are somewhat different. The IPSL projection produces again the strongest decline in biomass. It is a very consequent decrease with a biomass divided by 5 between the beginning and the end of the century. The two others projections have similar trends with less abrupt decline but still a reduction of 50% at the end of the time series.

The mechanisms leading to these changes have been investigated. The main driver was quickly identified and associated to the changes in the conditions defining the spawning habitat. With the warming of surface waters, where spawning and larvae development occur, a large proportion of the current spawning habitat becomes less and less favorable, i.e., upper the limit of estimated favorable spawning temperature range, especially in the equatorial Pacific warm pool and the eastern equatorial Indian Ocean. IPSL predicts the strongest temperature increase in these regions and consequently the largest decline in

larval recruits and then population biomass (see Figure 5). Additional simulations were conducted using average climatological series, i.e., the current average conditions, to replace separately the environmental variable SST, Primary production (PP), temperature in vertical layers and dissolved oxygen concentration (see Figure 27). The results confirm that without a SST increasing trend the stock would maintain and even increase its biomass (without fishing) in the Pacific Ocean. With much lower impacts, the decrease of primary production in the Indian Ocean has a negative impact while the warming of vertical layers in the Pacific ocean has a small positive impact. Note that these simulations do not take into account the species adaptation to a warmer spawning and juvenile temperatures ([Lehodey et al., 2015]), which may mitigate the predicted decline of the population biomass.

These results still need to be complemented by the analysis of possible drifts in the coupled physical-biogeochemical simulations. This will be investigated using reference control simulations. Then the influence of ocean acidification associated to the absorption by the ocean of a large quantity of CO2 released in the atmosphere by anthropogenic activity needs to be explored.

List of Tables

7 Tables

Table 1: Skipjack Fishing Dataset 2014. Definition of SEAPODYM fisheries in Pacific Ocean.

ID	Description	Nation	Resolution	Time period
P1	Sub-tropical pole-and-line	Japan	1°, month	1972 - 2012
P21	Pole-and-line	Japan	1°, month	1972 - 1982
P22	Pole-and-line	Japan	1°, month	1982 - 1990
P23	Pole-and-line	Japan	1°, month	1990 - 2012
P3	Tropical pole-and-line	Pacific Islands	1°, month	1970 - 2012
S4	Sub-tropical purse-seine	Japan	1°, month	1970 - 2012
S5	PS anchored FADs, WCPO	ALL	1°, month	1967 - 2012
S6	Purse-seine	Philippines, Indonesia	1°, month	1986 - 2010
S7	PS free schools, WCPO	ALL	1°, month	1967 - 2012
L8	Longline, WCPO	ALL	5°, month	1950 - 2012
L9	Longline, Domestic fisheries	Philippines, Indonesia	5°, month	1970 - 2011
S10	PS FADs, EPO	ALL	1°, month	1996 - 2013
S11	PS LOGs, EPO	ALL	1°, month	1996 - 2013
S12	PS Animal associations, EPO	ALL	1°, month	1996 - 2013
S13	PS Free schools, EPO	ALL	1°, month	1996 - 2013
S14	PS Unknown log, EPO	ALL	1°, month	1996 - 2013
P15	Pole-end-line, EPO	ALL	5°, month	1972 - 2008

Table 2: Forcing variables used in current SEAPODYM application. Note that all variables were interpolated onto SEAPODYM grid with the resolution shown for micronekton variables.

Code	Variable	Description	Resolution	Time period
		Physical forcing		
NEMO	T, u, v	Ocean reanalysis, NEMO general circulation model with ERA-interim atmospheric forcing	ORCA2, 30 days	1/1979 -12/2010
		Biogeochemical forcing		
PISCES	PP, Z, $O2$	Primary production, euphotic depth and oxygen predicted by PISCES model coupled to NEMO-INTERIM	ORCA2, 30 days	1/1979 -12/2010
		Biological forcing		
MTL	F	Six micronekton groups predicted by SEAPODYM-MTL model	1°, 30 days	1/1979 -12/2010

Table 3: Configuration of optimization experiments.

ID	**Catch prediction method**	**Data in the likelihood**
E1	Effort-based for PL, catch removal for PS	Catch, LF
E2	Catch removal for all fisheries	Catch, LF, tags
E3	Effort-based for PL, Catch removal for PS	Catch, LF, tags

Table 4: Parameter estimates from three optimization experiments: E1 - population model with likelihood with fishing data only, E2 - full model configuration, including tagging data in the likelihood and catch predicted without effort for all fisheries and E3 - full model configuration with tagging data likelihood, but pole-and-line fisheries catches are predicted based on fishing effort. Parameters marked by asterisks were fixed in optimization experiment. Parameter with [or] were estimated at their lower or upper boundary correspondingly. The dash indicates that the parameter is not effective.

θ	**Description**	**E1**	**E2**	**E3**
	Reproduction			
σ_0	standard deviation in temperature Gaussian function at age 0, $^\circ C$	2.5]	1.37	1.48
$T_0^\star$	optimal surface temperature for larvae, $^\circ C$	28.52	28.96	[28.5
α_P	prey encounter rate in Holling (type III) function, day^{-1}	0.015	1]	0.08
α_F	Log-normal mean parameter predator-dependent function, g/m^2	1.86	2.5]	2.48
β_F	Log-normal shape parameter in predator-dependent function	1.7	1.9	2.5
R	reproduction rate in Beverton-Holt function, mo^{-1}	0.027	0.25]	0.2
b	slope parameter in Beverton-Holt function, nb/km^2	1]	0.17	0.49
	Mortality			
$\bar{m}_p$	predation mortality rate age age 0, mo^{-1}	0.3*	0.25*	0.25*
β_p	slope coefficient in predation mortality	0.38	[0.05	[0.05
$\bar{m}_s$	senescence mortality rate at age 0, mo^{-1}	0.0035]	0.0025	0.0099
β_s	slope coefficient in senescence mortality			
ϵ	variability of mortality rate with habitat index $M_H \in (\frac{M}{(1+\epsilon)}, M(1+\epsilon))$	[0.1	[0	[0
	Habitats			
T_0	optimal temperature (if Gaussian function), or temperature range for the first young cohort, $^\circ C$	31]	31.1]	31.1]
T_K	optimal temperature (if Gaussian function), or temperature range for the oldest adult cohort, $^\circ C$	26]	26.05]	25.9319
γ	slope coefficient in the function of oxygen)	[1e-05	[1e-06	[1e-6
$\hat{O}$	threshold value of dissolved oxygen, ml/l	3.5	3.6548	3.6424
eF_1	contribution of epipelagic forage to the habitat	[0.5	4]	4]
eF_1	contribution of mesopelagic forage to the habitat	[2.0001	0.05*	0.05*
eF_1	contribution of migrant mesopelagic forage to the habitat	[0.5	[0	[0
eF_1	contribution of bathypelagic forage to the habitat	[0*	[0*	[0*
eF_1	contribution of migrant bathypelagic forage to the habitat	[2e-04	[0*	[0*
eF_1	contribution of highly migrant bathypelagic forage to the habitat	[0.5	1.664	1.8914
	Movement			
V_m	maximal sustainable speed of tuna in body length, BL/sec	[0.85	0.5912	0.7766
a_V	slope coefficient in allometric function for maximal speed	1.1]	[0.4	0.8349
σ	multiplier for the maximal diffusion rate	0.155]	0.2]	0.2]
c	coefficient of diffusion variability with habitat index	1]	0.9362	0.9414

Table 5: Predicted proportions of skipjack biomass at life stage by optimization experiment and region (NPO - north of 10N, EqPO - between 10S and 10N and SPO - south of 10S).

Life stage	**Region**	**E1**	**E2**	**E3**
	NPO	23%	11%	17%
Larvae 0-3mo	EqPO	57%	78%	67%
	SPO	21%	11%	17%
	NPO	25%	13%	18%
Young	EqPO	54%	79%	69%
	SPO	21%	8%	13%
	NPO	27%	15%	18%
Adults	EqPO	50%	72%	68%
	SPO	23%	13%	14%

List of Figures

8 Figures

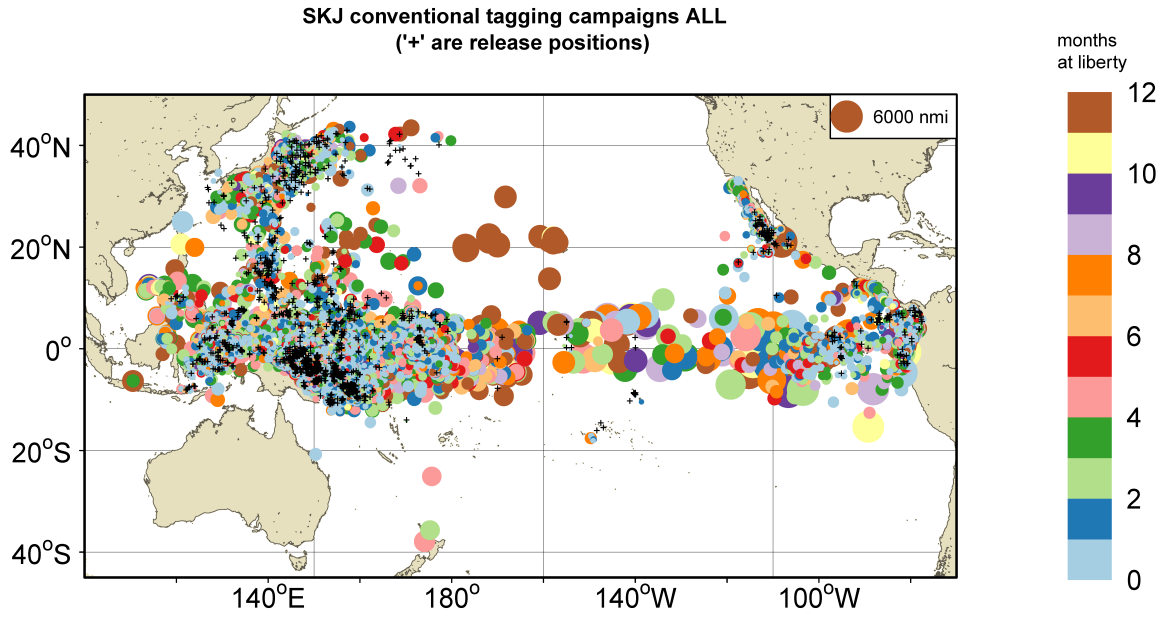

Figure 6: All available conventional tagging data.

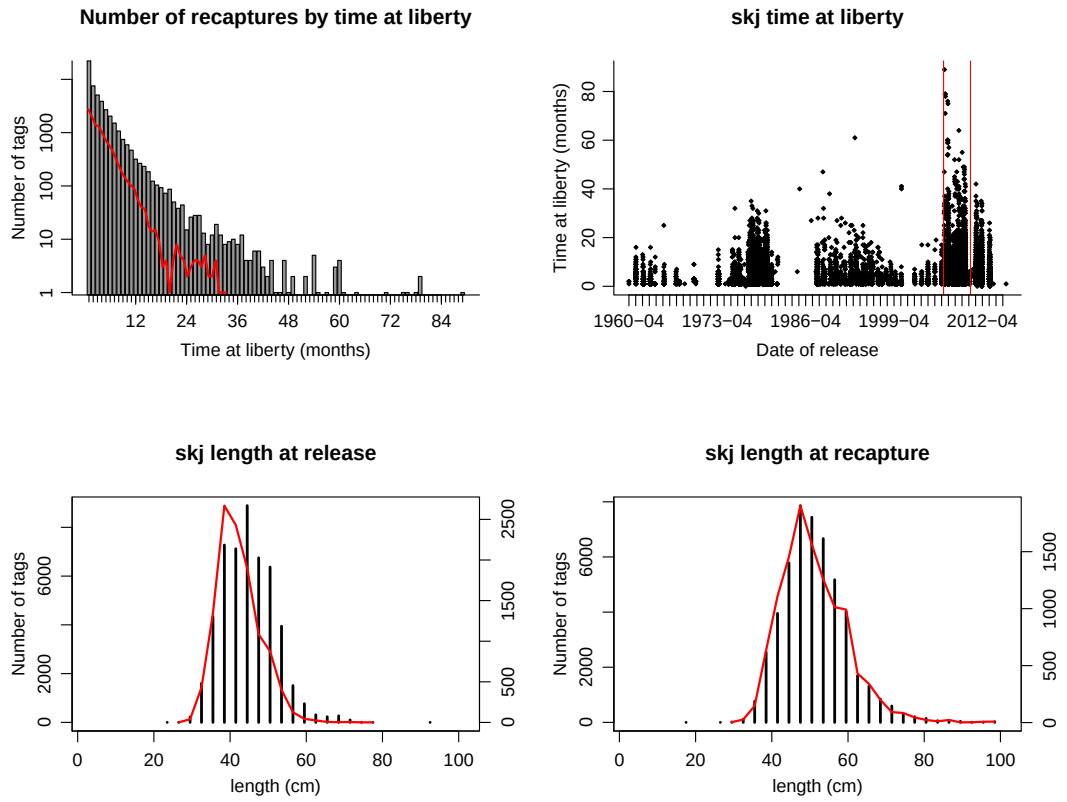

Figure 7: Available conventional tagging (black bars and dots) and the data being used in optimization (red lines): (top) time at liberty histogram and time at liberty of the tags depending on their date of release; (bottom) size distribution at release and recapture.

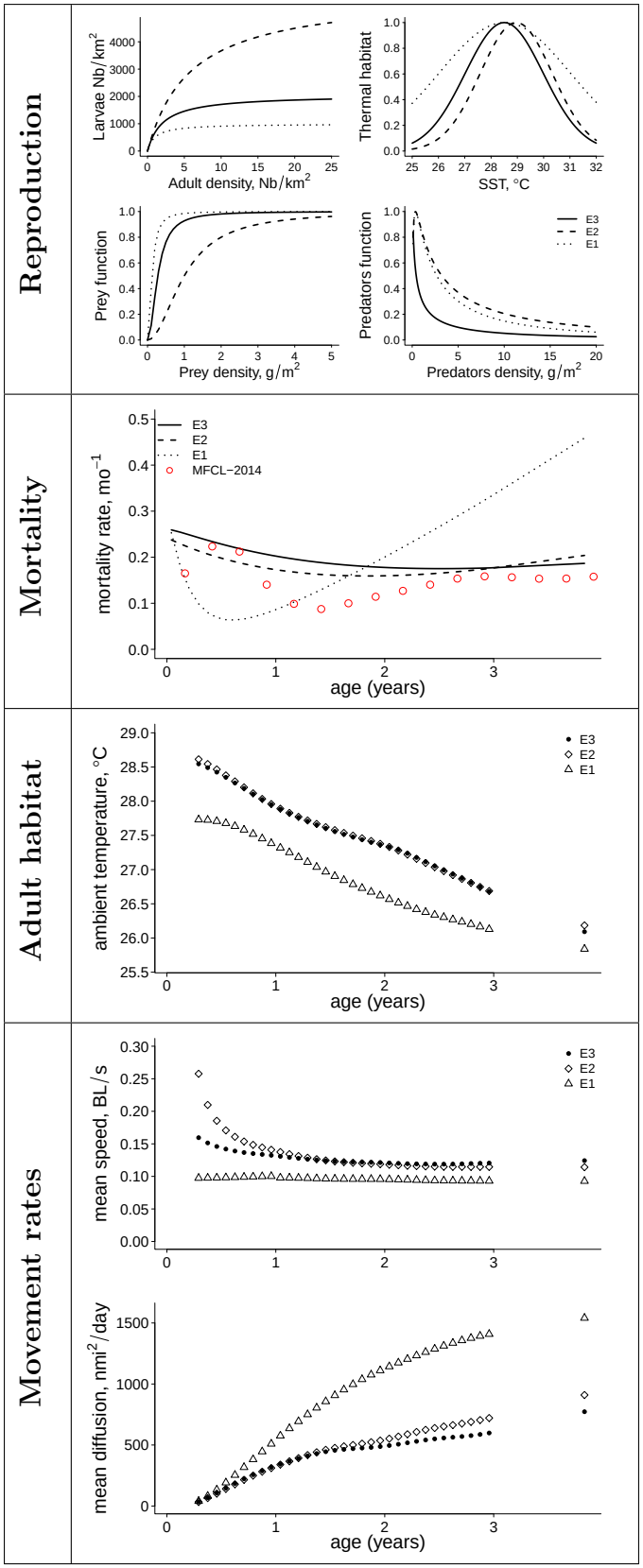

Figure 8. Estimated parameters in the optimization experiments E1, E2 and E3. Evolution of main model parameters through population life history: topleft - preferred habitat temperature; topright - average mortality rates; bottomleft - mean speed in body length and bottomright - mean diffusion rate

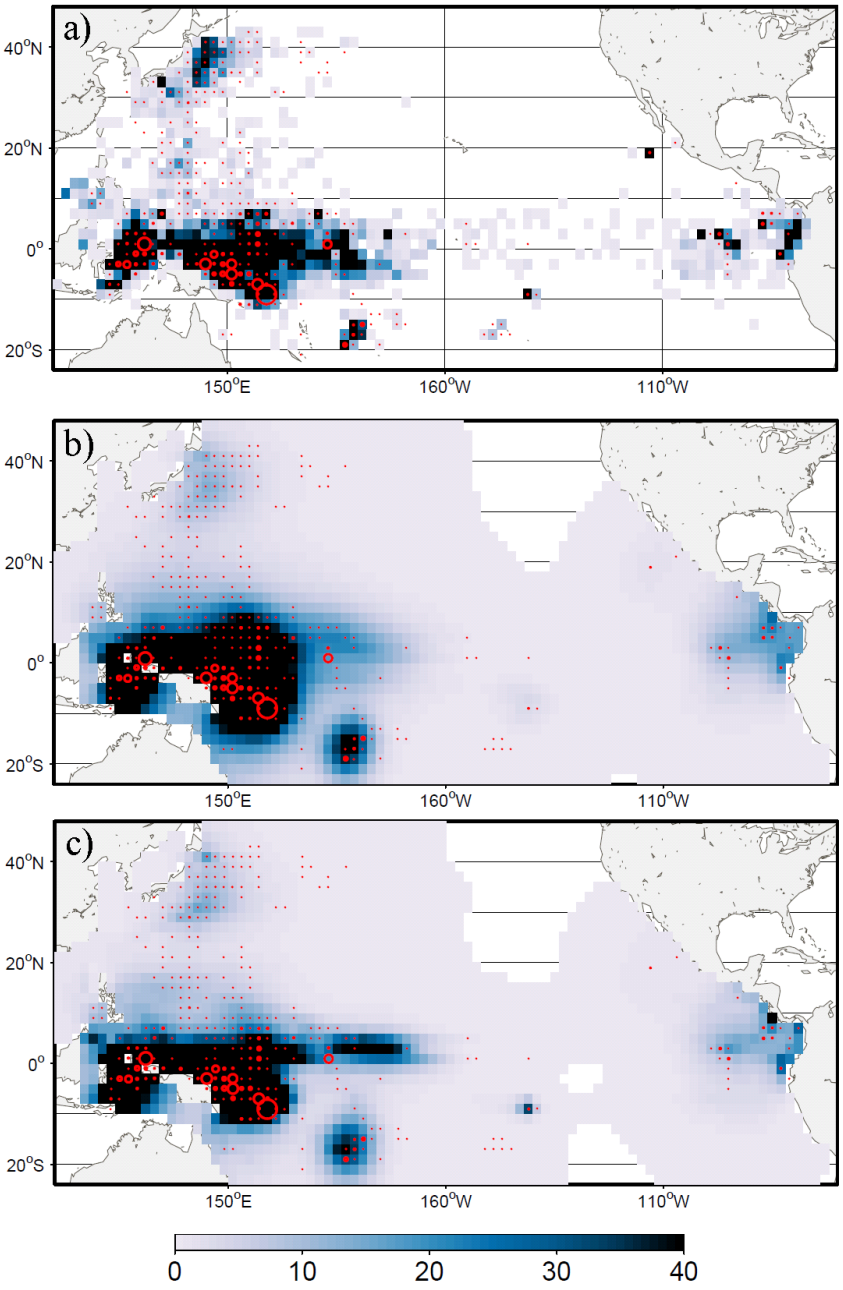

Figure 9: Maps of tag recaptures observed (a) and predicted by SEAPODYM with parameter estimates of E1 (b) optimization experiment with fishing data likelihood and E2 (c), the experiment with full likelihood including tagging data. Validation runs configured to include all tagging data over the simulation period 1979-2010. The red circles show the release positions.

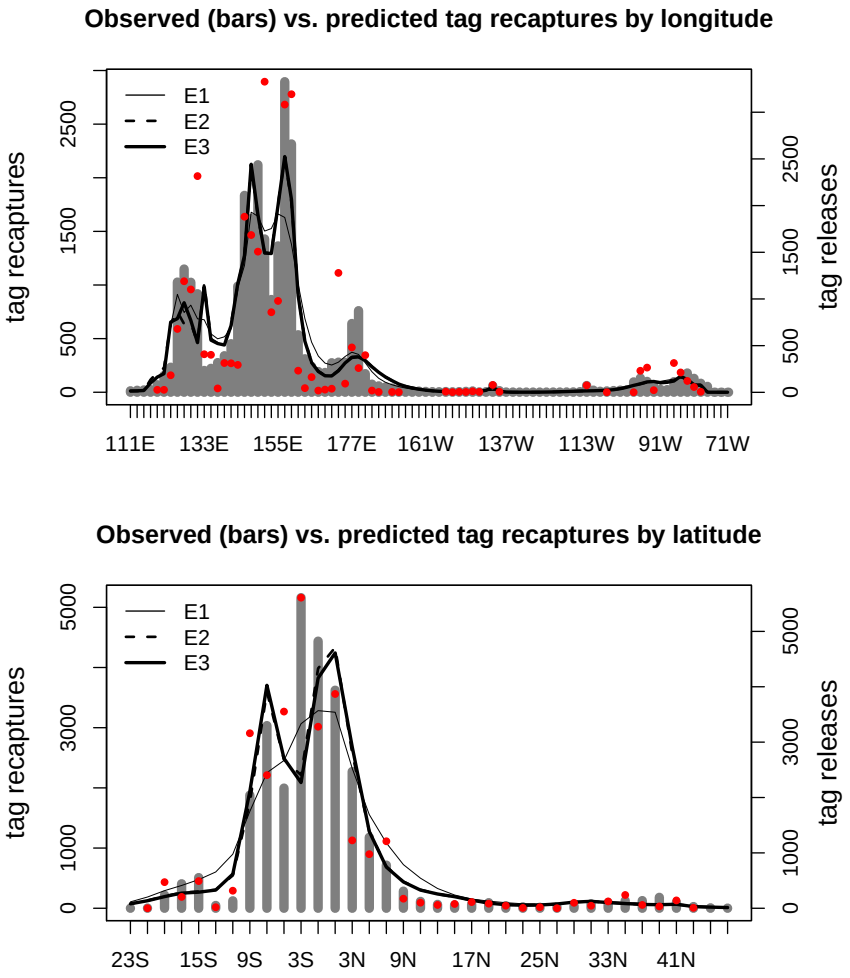

Figure 10: Comparison of observed and predicted tag recapture distributions as the solutions of E1 and E2 optimization experiments: (top) longitudinal and (bottom) latitudinal profiles. Red dots show the number of releases. On the left - the result of full likelihood estimation, on the right - only tagging data in the likelihood.

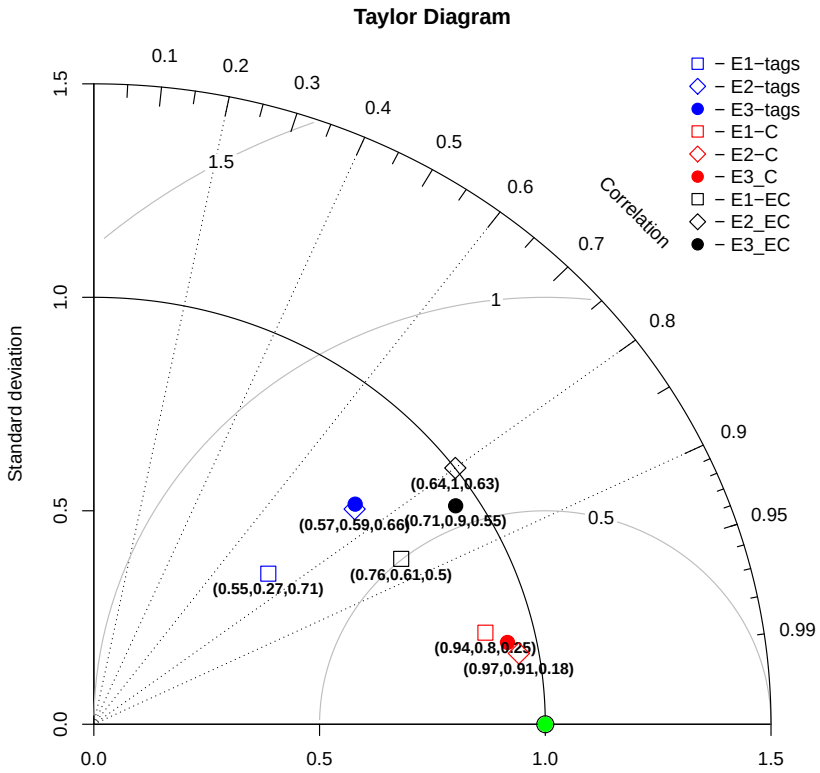

Figure 11: Taylor diagram, providing three aggregated metrics of model fit to the data: correlation (angular coordinates) between predictions and observations, standard deviation ratio (distance from (0,0) point depicts the ratio between model and data standard deviation) and normalized mean squared error (concentric circles with the green bullet being the center). Three points for each optimization experiment show the metrics of the fit to the tag recapture data (E1-tags and E2-tags), catch data predicted using catch removal method (E1-C and E2-C) and catch data predicted using fishing effort (E1-EC and E2-EC).

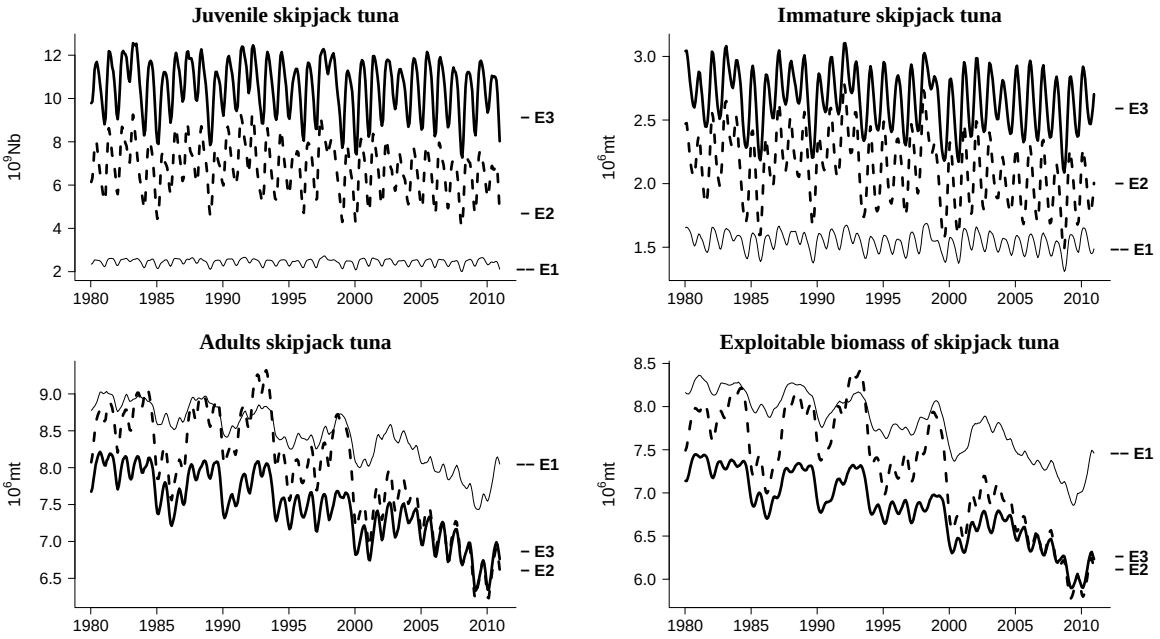

Figure 14: Time series of (from top to bottom and left to right) juvenile (0-3 months of age), young, adult and total exploitable biomass of skipjack. The time series are extracted over the region (130E-70W,40S-45N).

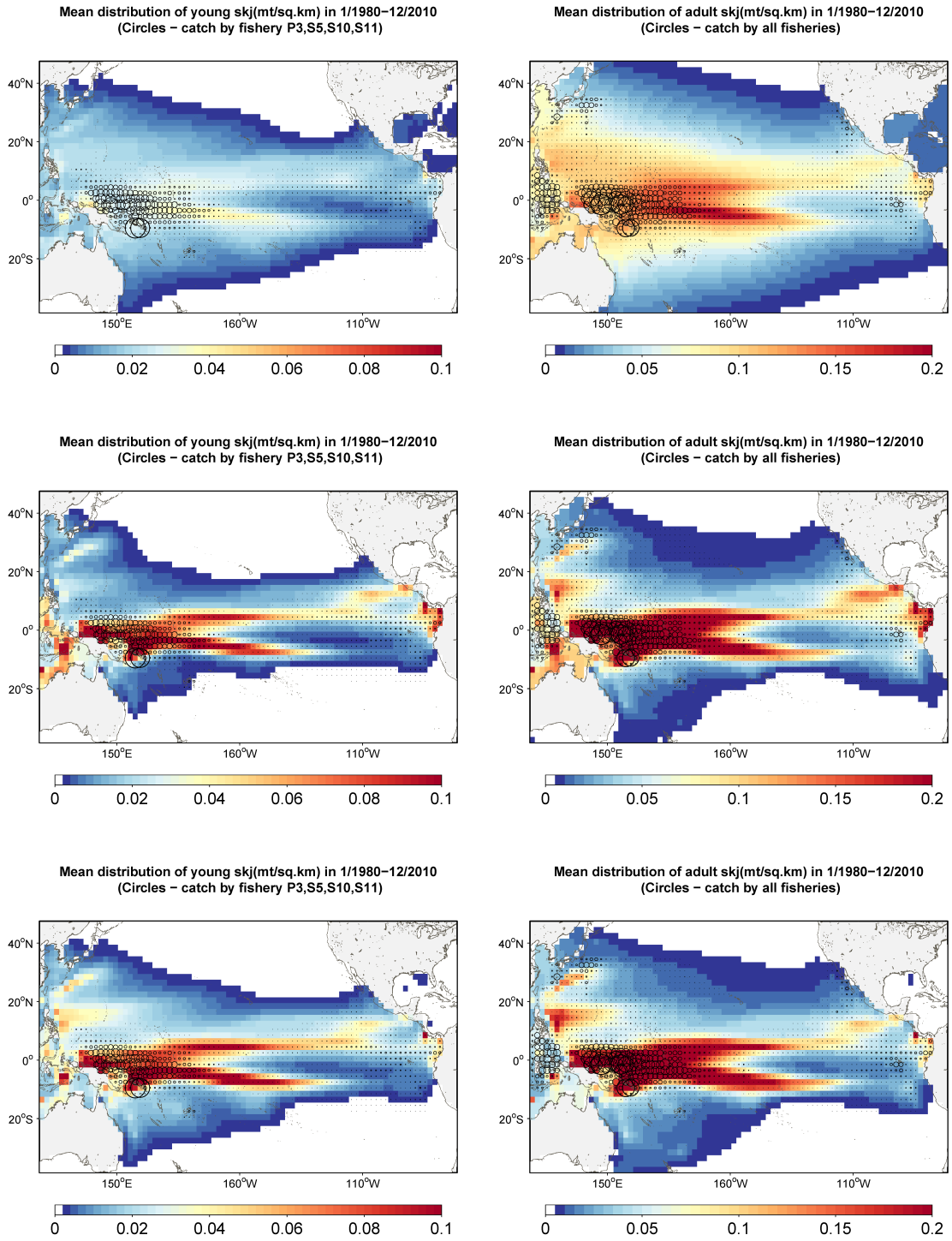

Figure 12: Average spatial distributions of young (left) and adult (right) biomass predicted by (from top to bottom) E1, E2 and E3 experiments.

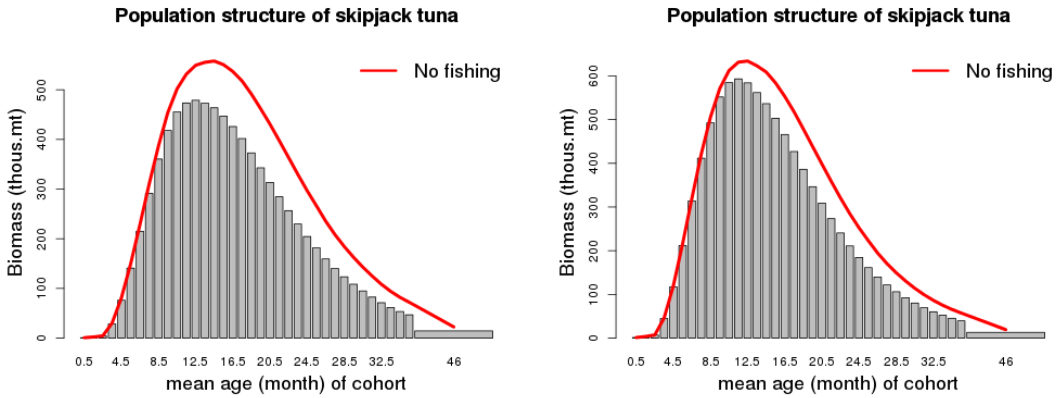

Figure 13: Population composition by age: (left) predicted with E2 solution, (right) predicted with E3 solution. Red line depict the population structure without fishing.

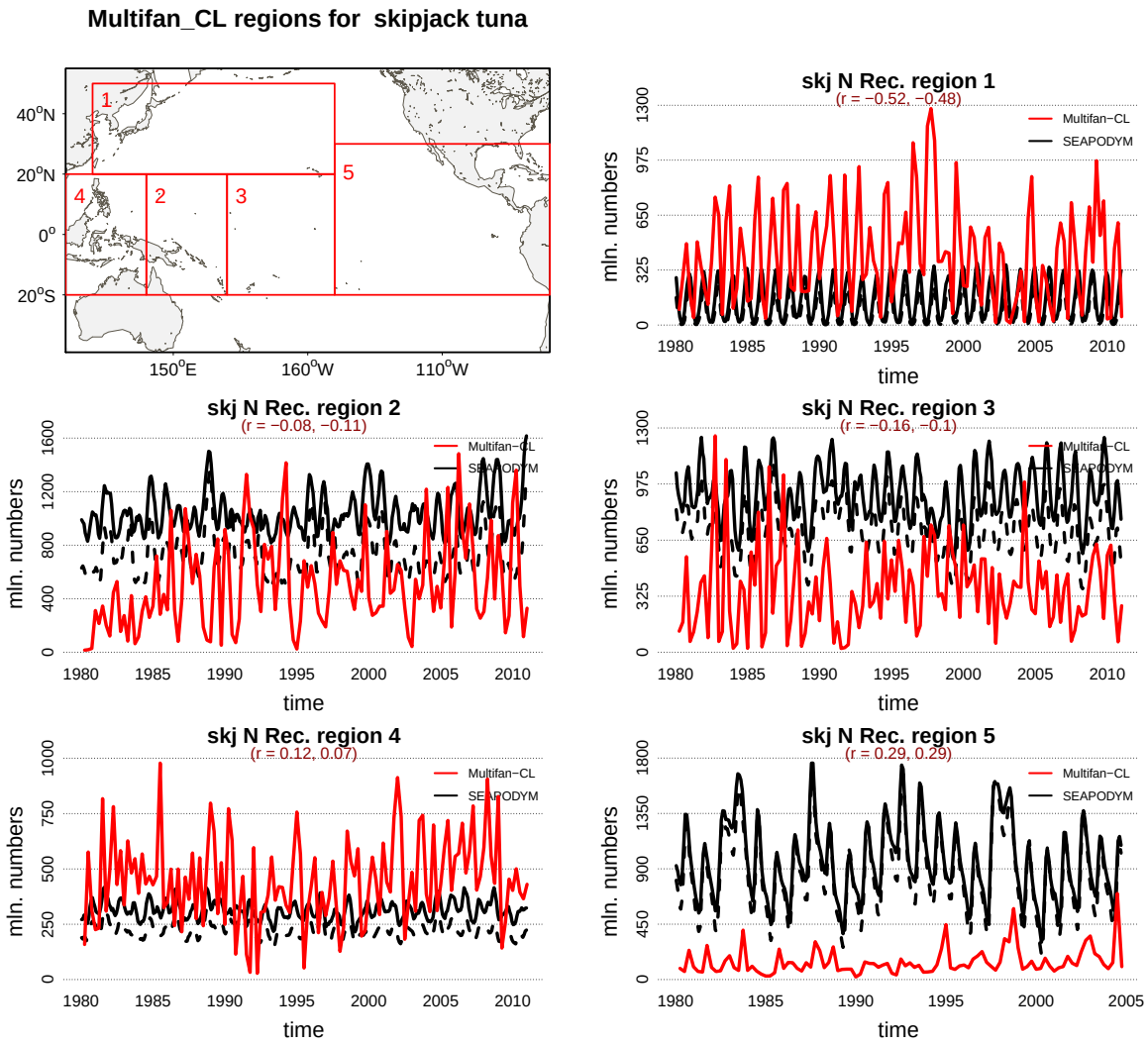

Figure 15: Regional comparison between SEAPODYM and Multifan-CL model predictions for recruitment. E2 is shown by dashed line, E3 - solid black line.

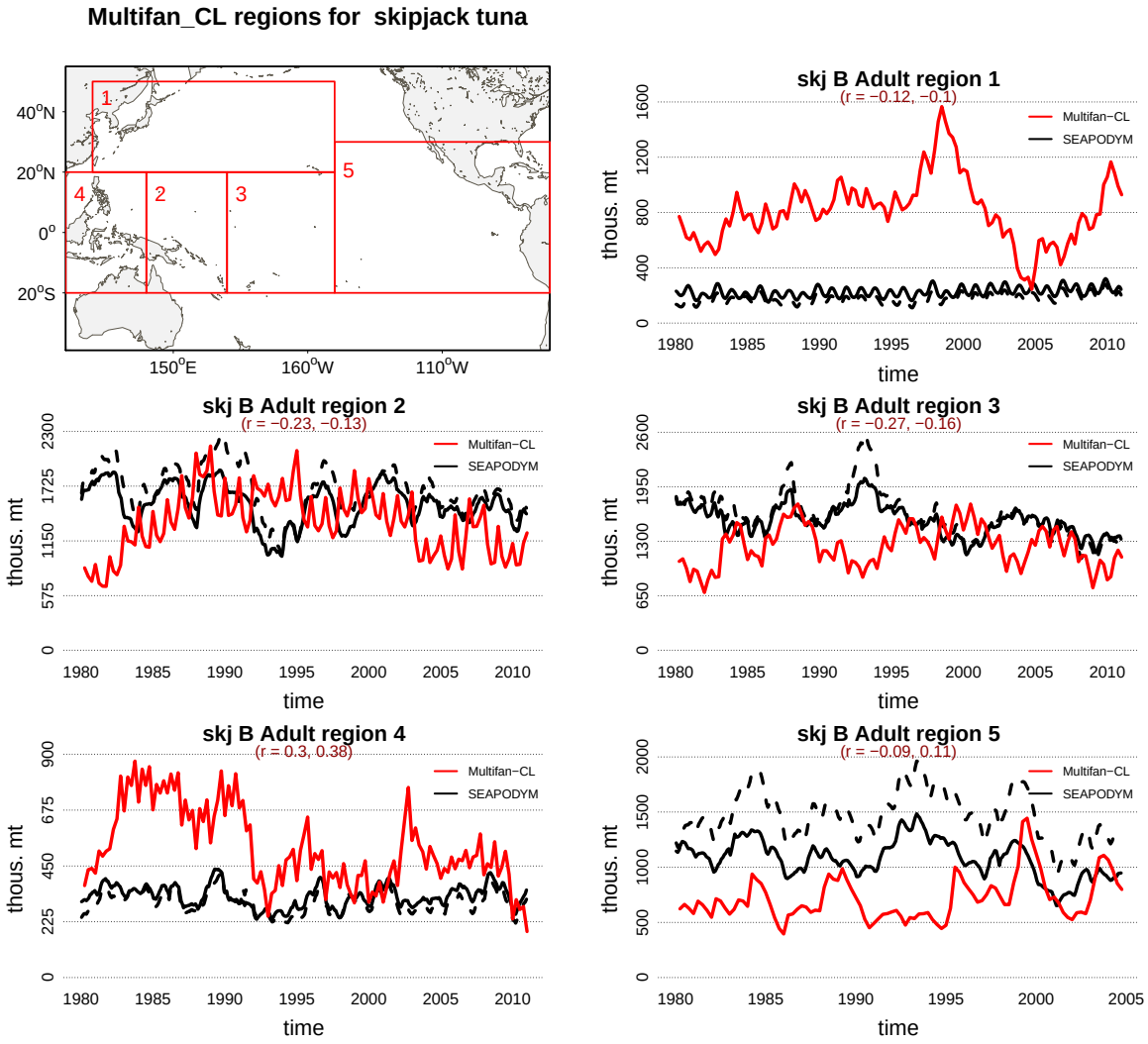

Figure 16: Regional comparison between SEAPODYM and Multifan-CL model predictions for spawning biomass. E2 is shown by dashed line, E3 - solid black line.

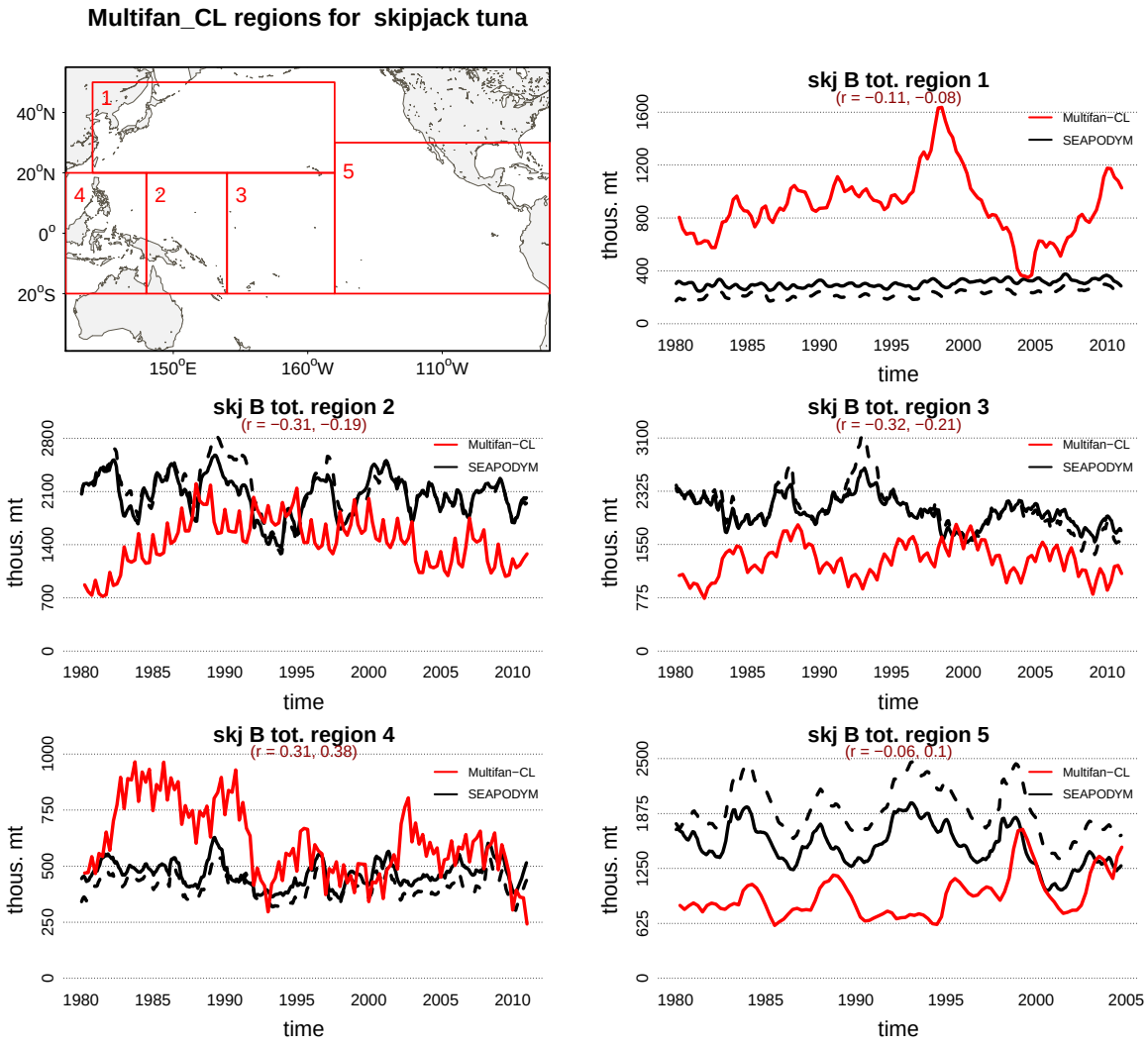

Figure 17: Regional comparison between SEAPODYM and Multifan-CL model predictions for total (immature and mature) biomass. E2 is shown by dashed line, E3 - solid black line.

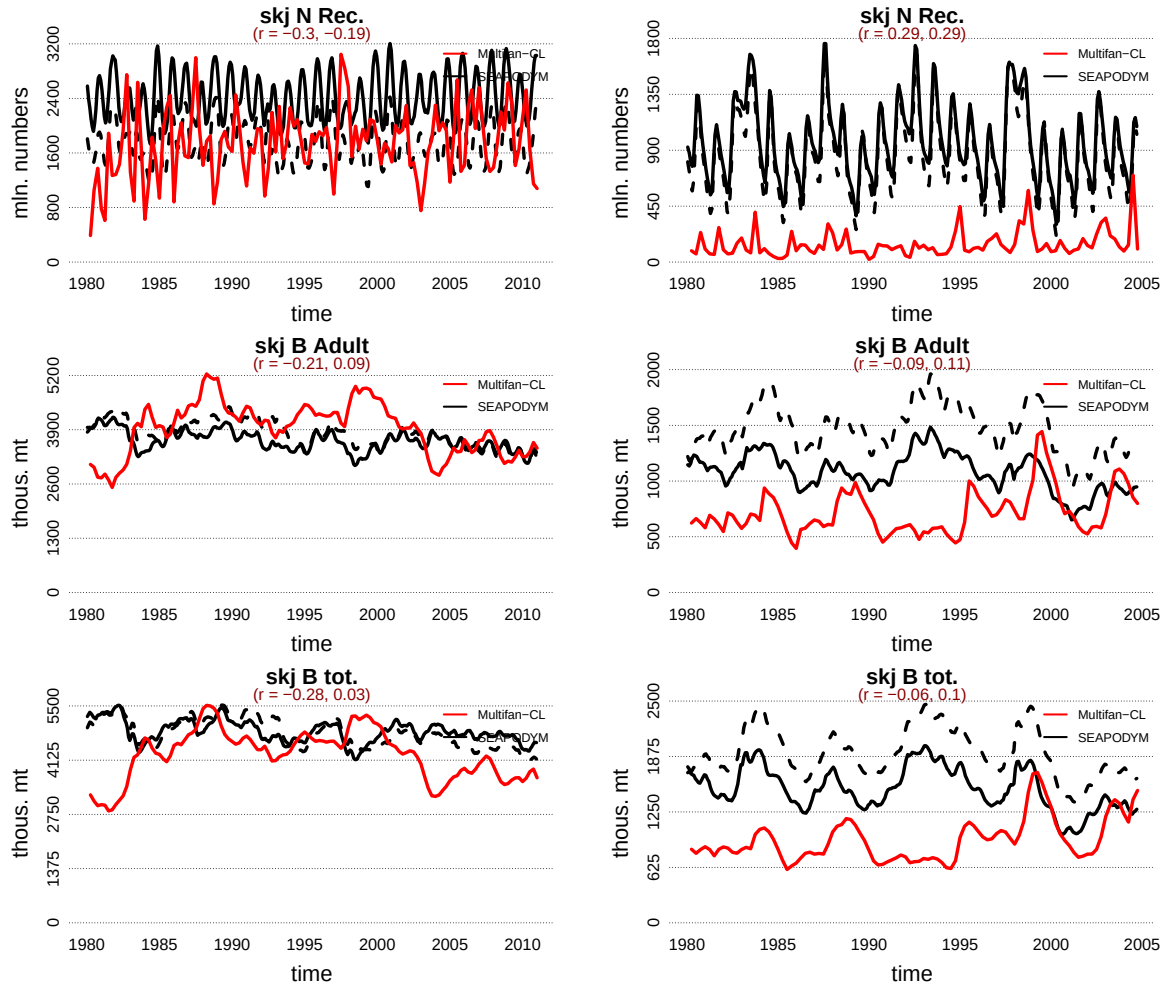

Figure 18: Comparison of (from top to bottom) recruitment, spawning and total biomass predicted by SEAPODYM and Multifan-CL models for WCPO (left) and EPO (right) (immature and mature) biomass. E2 is shown by dashed line, E3 - solid black line.

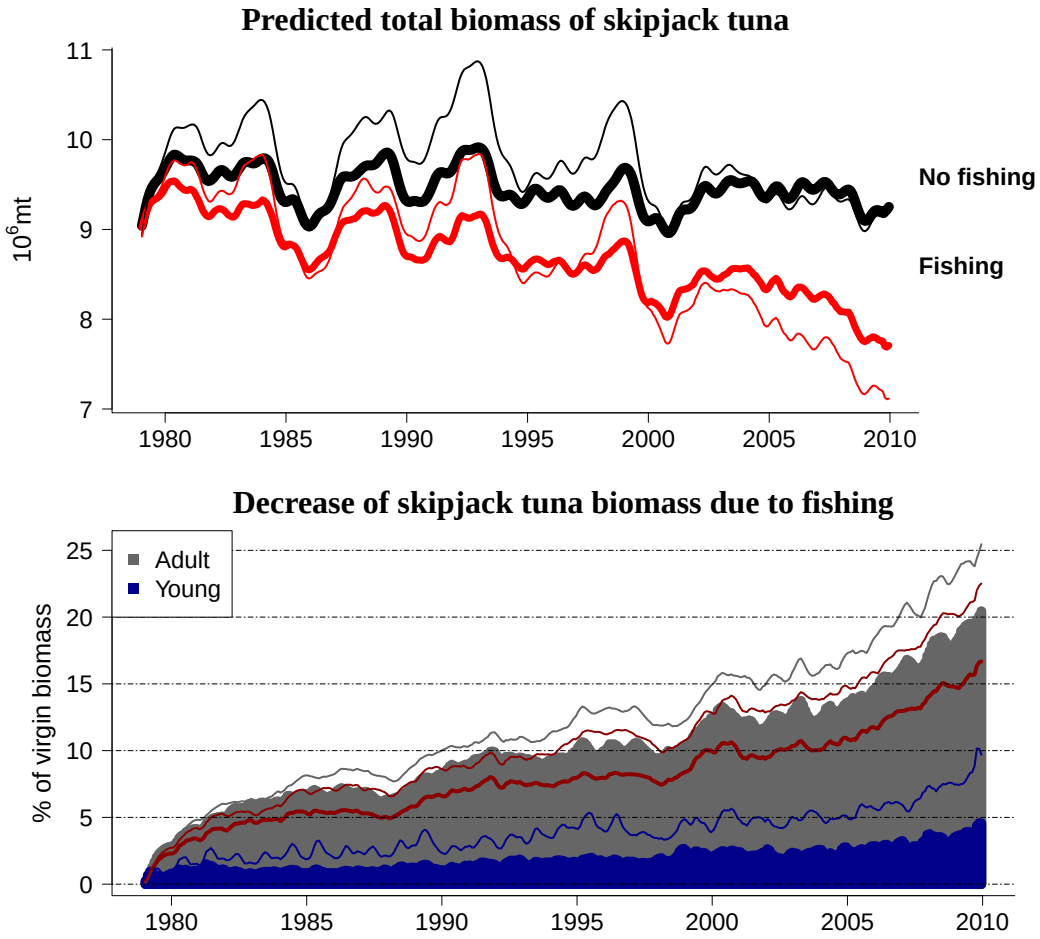

Figure 19: Quantification of fishing impact on young and adult population stages. Thin lines show the fishing impact estimation with the E2 solution, thick lines and shaded areas corresponds to the estimation with E3 run.

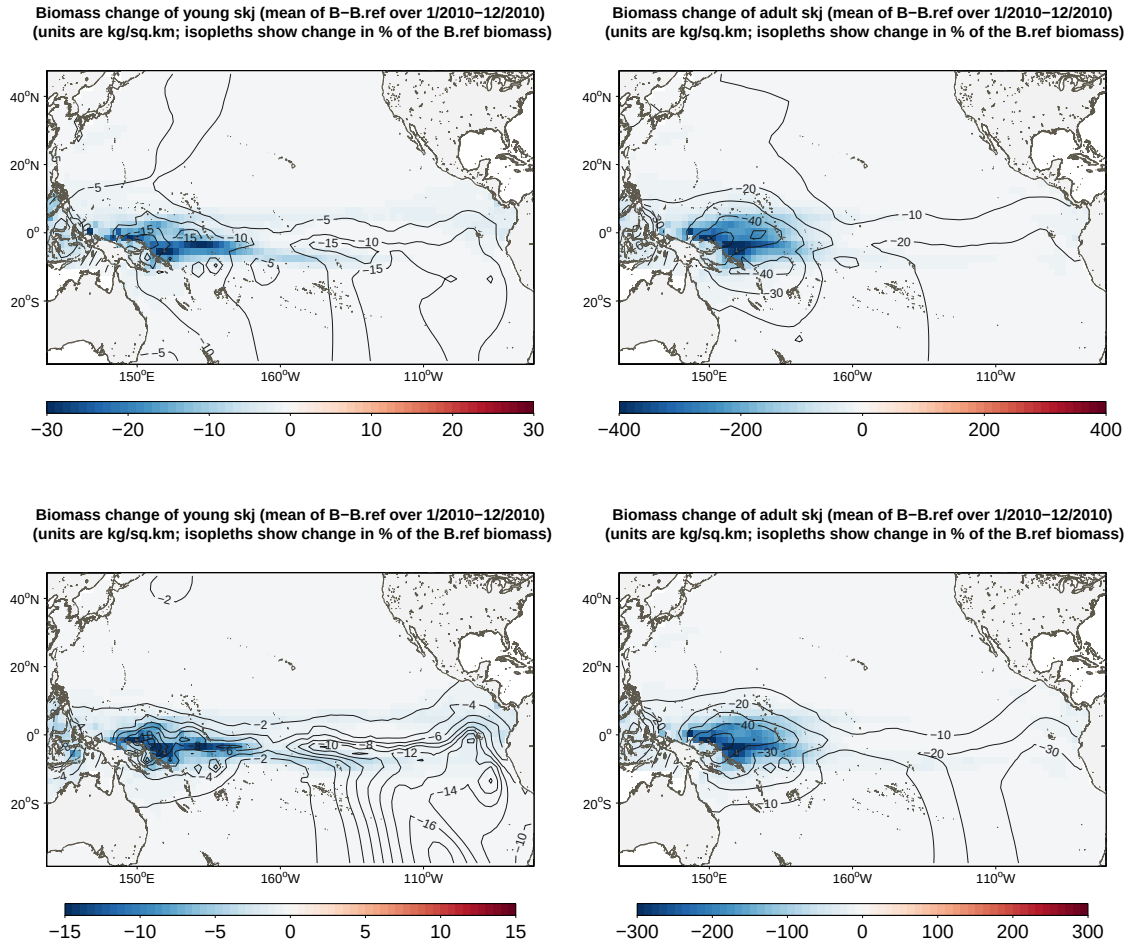

Figure 20: Spatial fishing impact on young and adult population stages for (top) E2 and (bottom) E3. Contour lines show the index $\frac{B_{F0}-B_{ref}}{B_{F0}}$ and colour shows the average biomass reduction due to fishing.

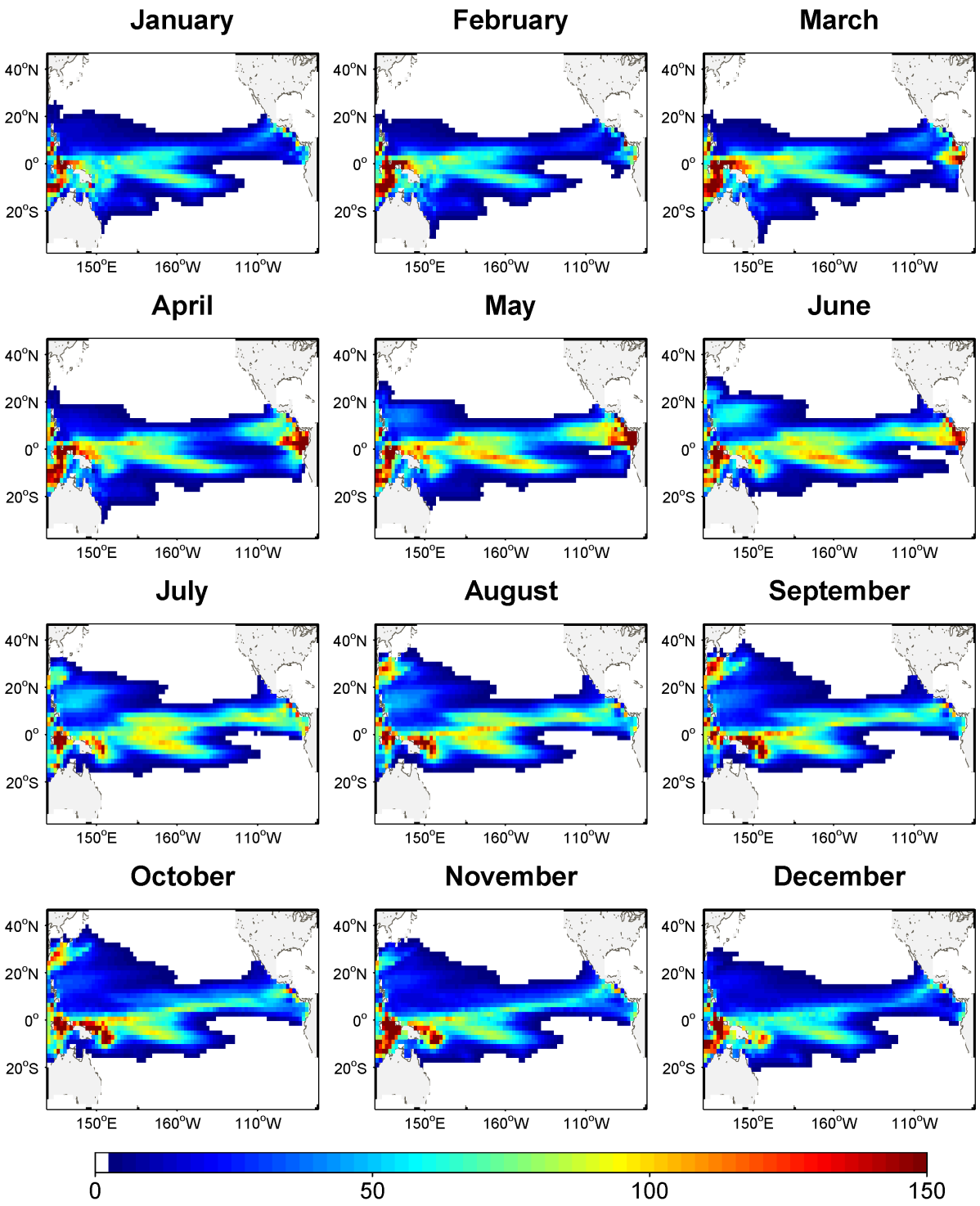

Figure 21: Mean monthly distributions of skipjack larvae (2001-2010 average) predicted by E2 solution.

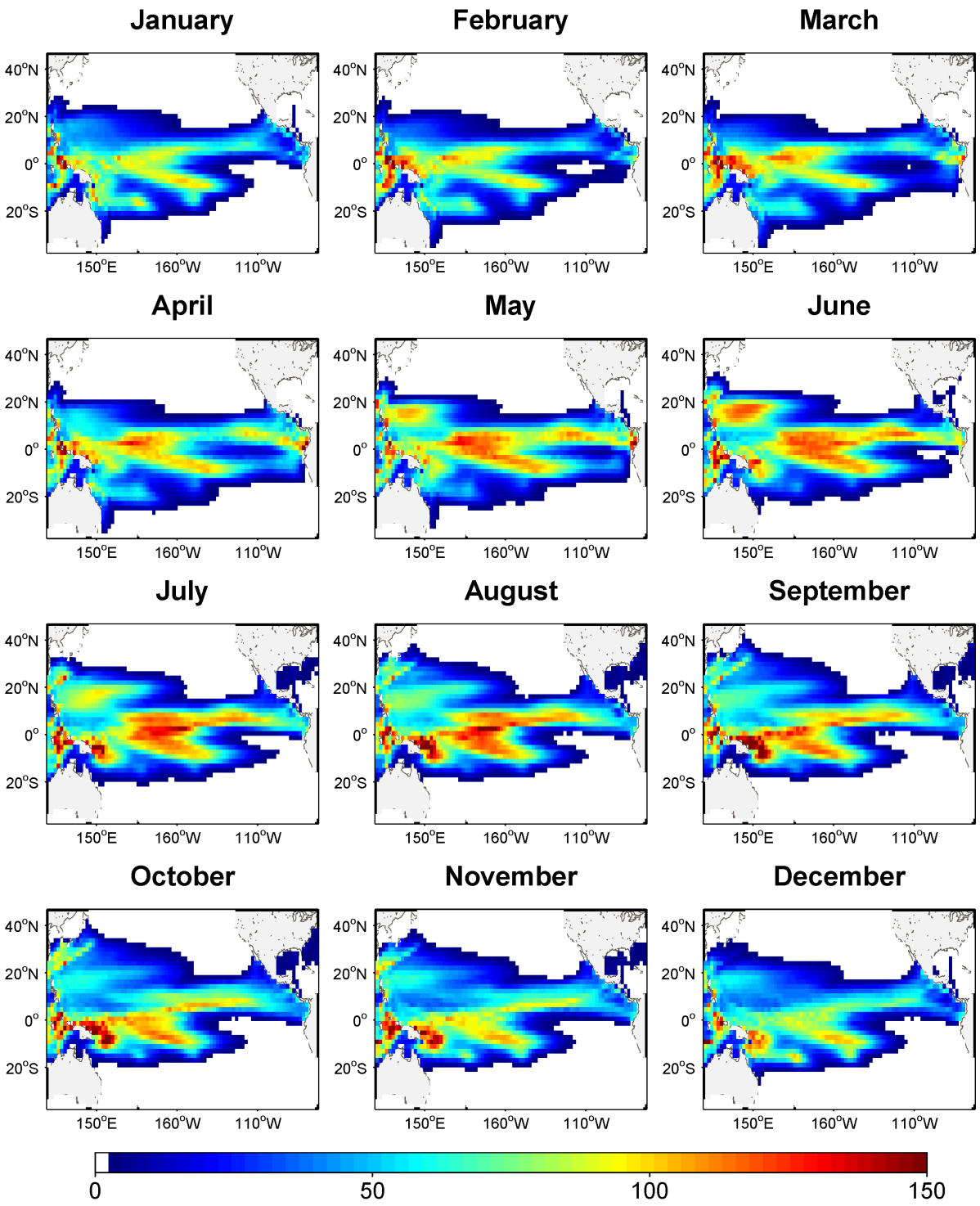

Figure 22: Mean monthly distributions of skipjack larvae (2001-2010 average) predicted by E3 solution.

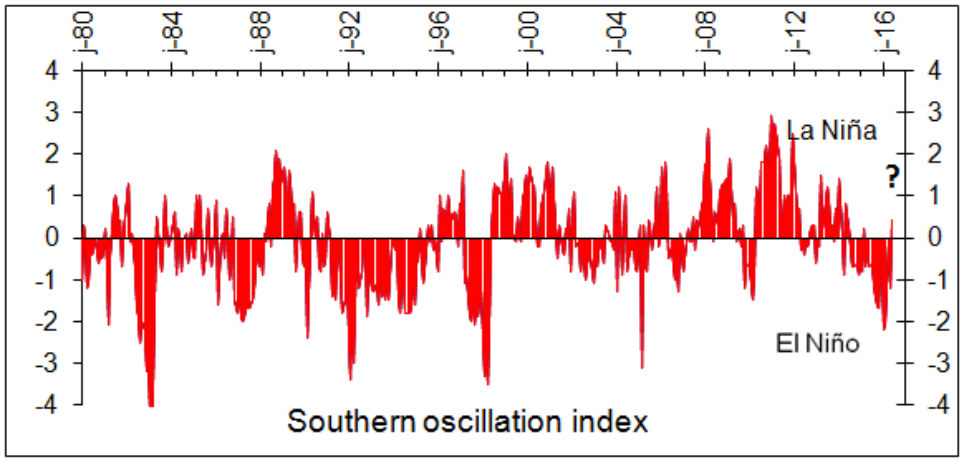

Figure 23: SOI Index since Jan 1980, data from http://www.cpc.ncep.noaa.gov/data/indices/soi.

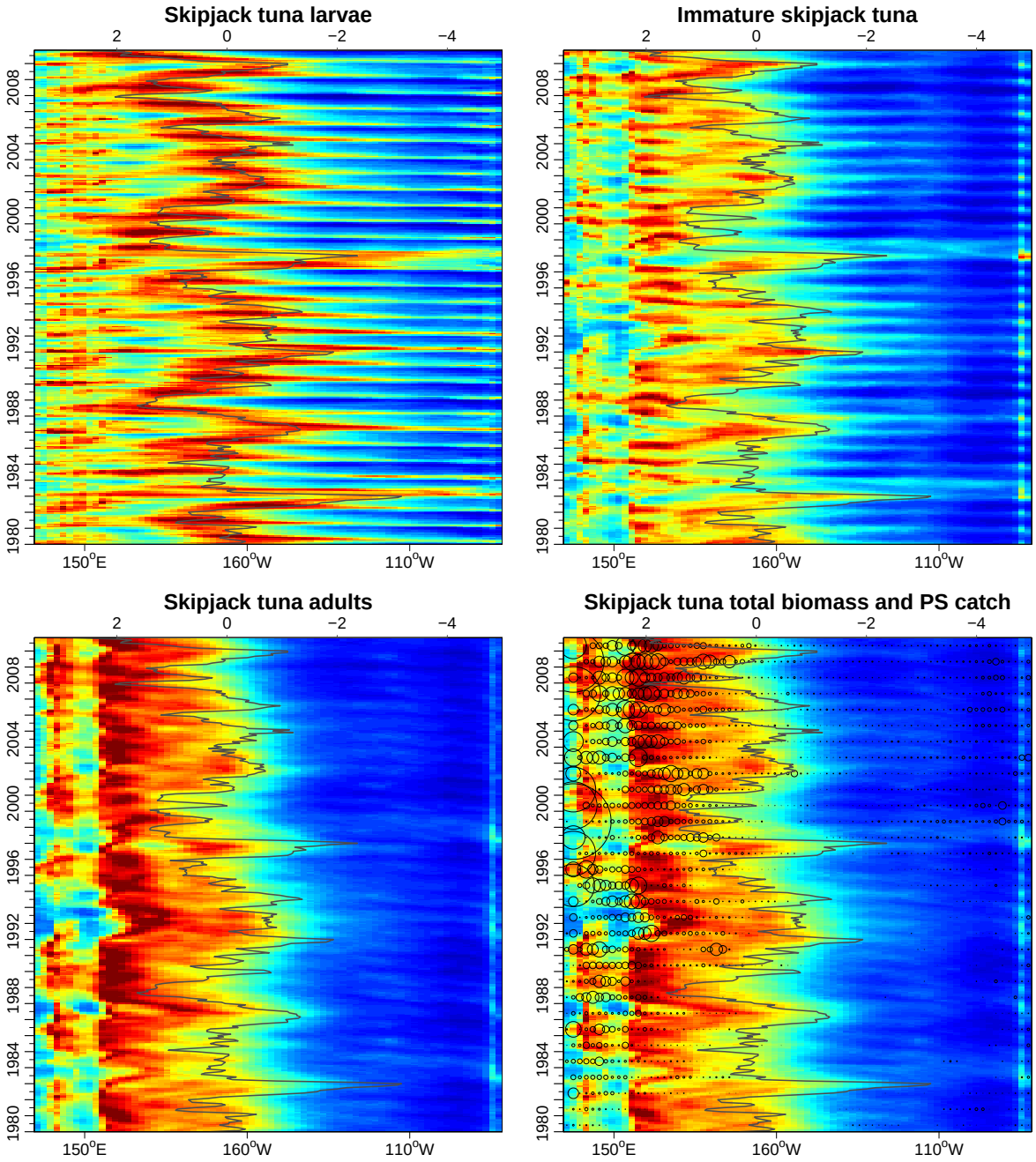

Figure 24: Variability of tropical (average over 10°S-10°N) biomass of larvae, young, adult skipjack and total (sum of young and adult) biomass, overlayed with three-months moving average of Southern Oscillation Index. The biomass distributions are shown with the color (blue - near zero values, dark red - maximal values); SOI (axis on the top of the map) dynamics is depicted by the solid line; circles show the purse-seine catches in 10°S-10°N area. Biomass predictions are derived from the experiment E3.

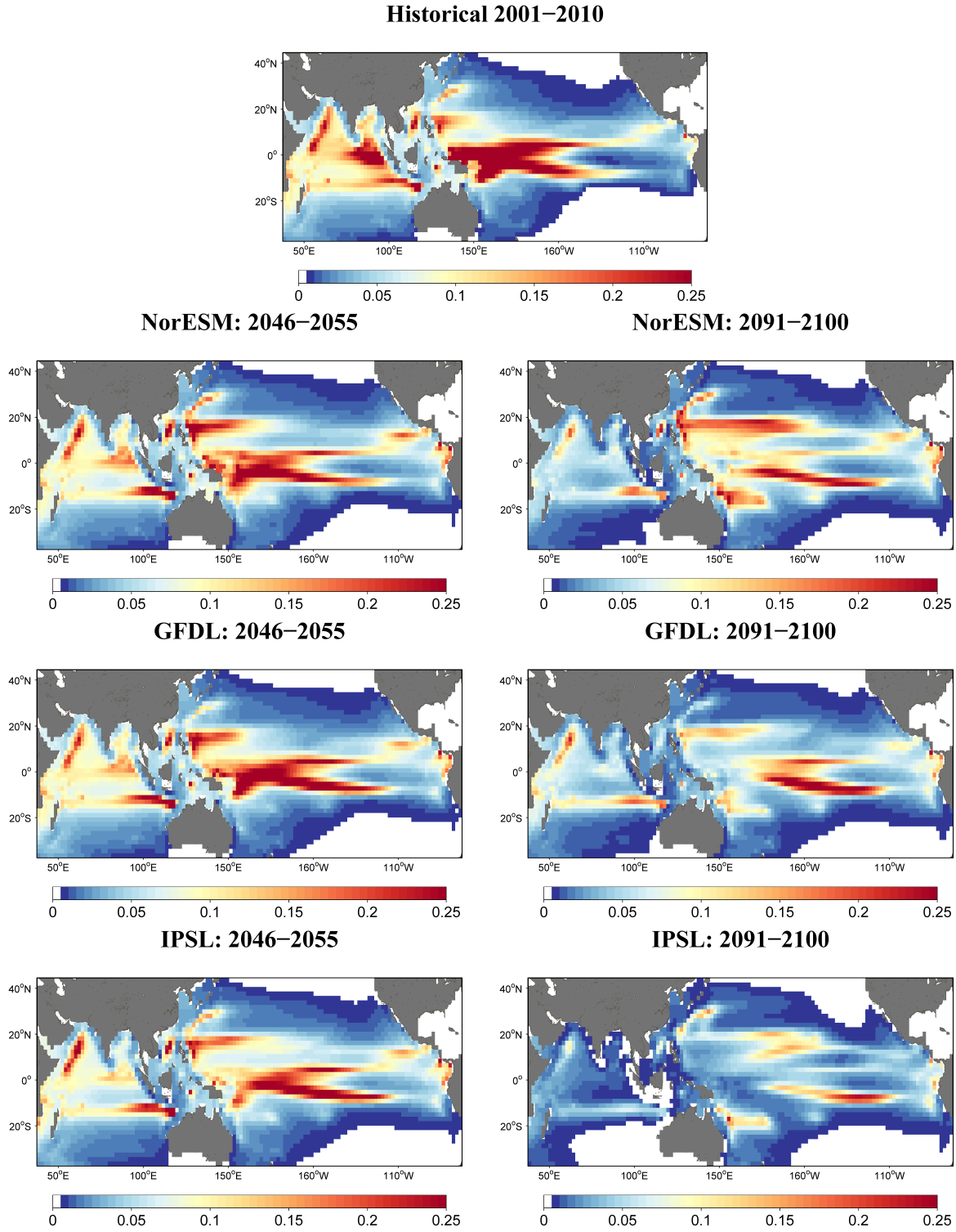

Figure 25: Biomass (mt/sq.km) of adult skipjack tuna predicted with INTERIM historical (2001-2010) and 3 different future climate forcings from 3 Earth Models under IPCC RCP8.5 scenario.

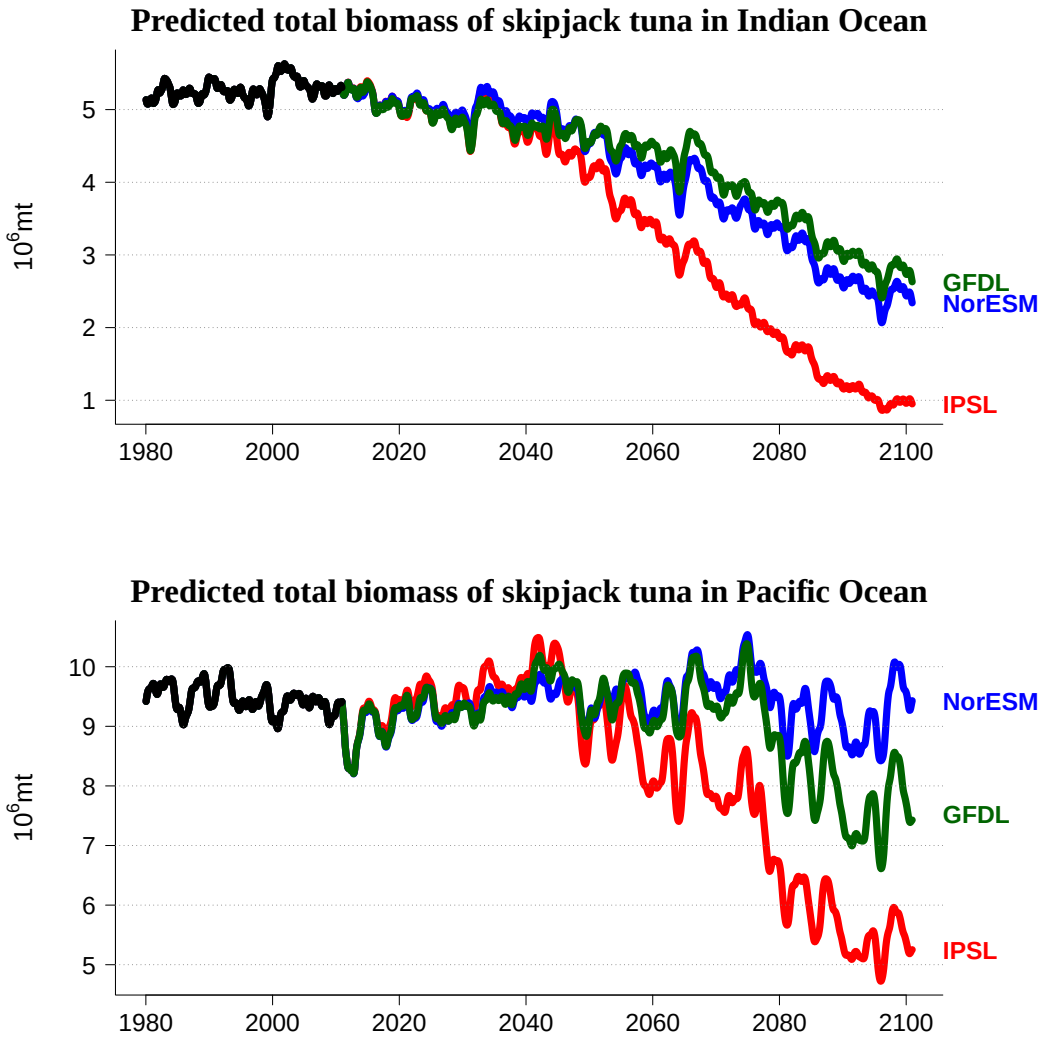

Figure 26: Predicted total biomass (historical simulation with fishing) and projected (without fishing) impact of climate change using atmospheric outputs from 3 different Earth Models under IPCC RCP8.5 scenario to drive the coupled physical-biogeochemical NEMO-PISCES model and then SEAPODYM.

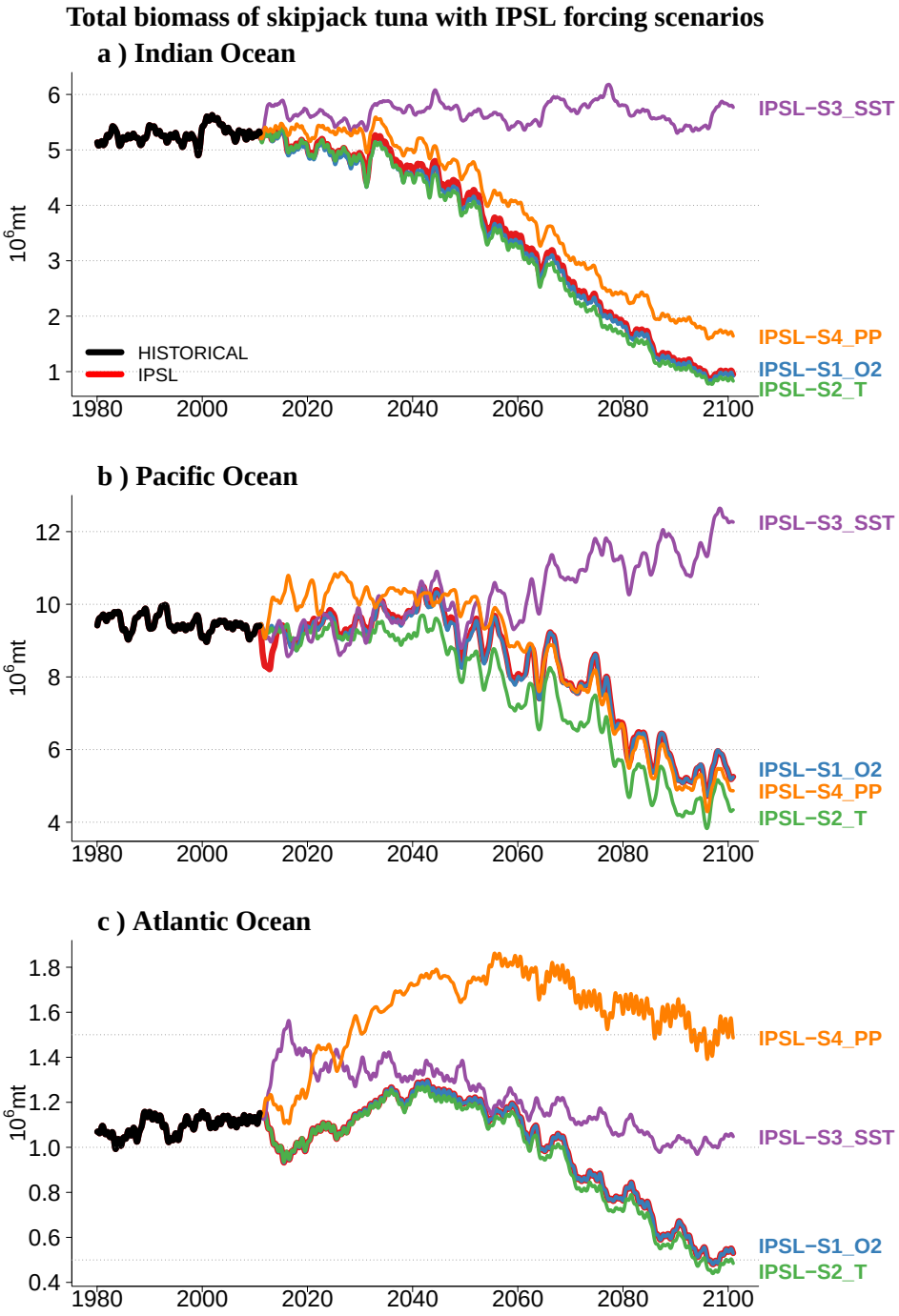

Figure 27: Predicted total biomass of skipjack during INTERIM reanalysis and IPSL projection period under IPCC RCP8.5 scenario. The four additional scenarios are shown:

A Appendices

A.1 Seapodym fisheries

A.2 Fit to the catch and LF data

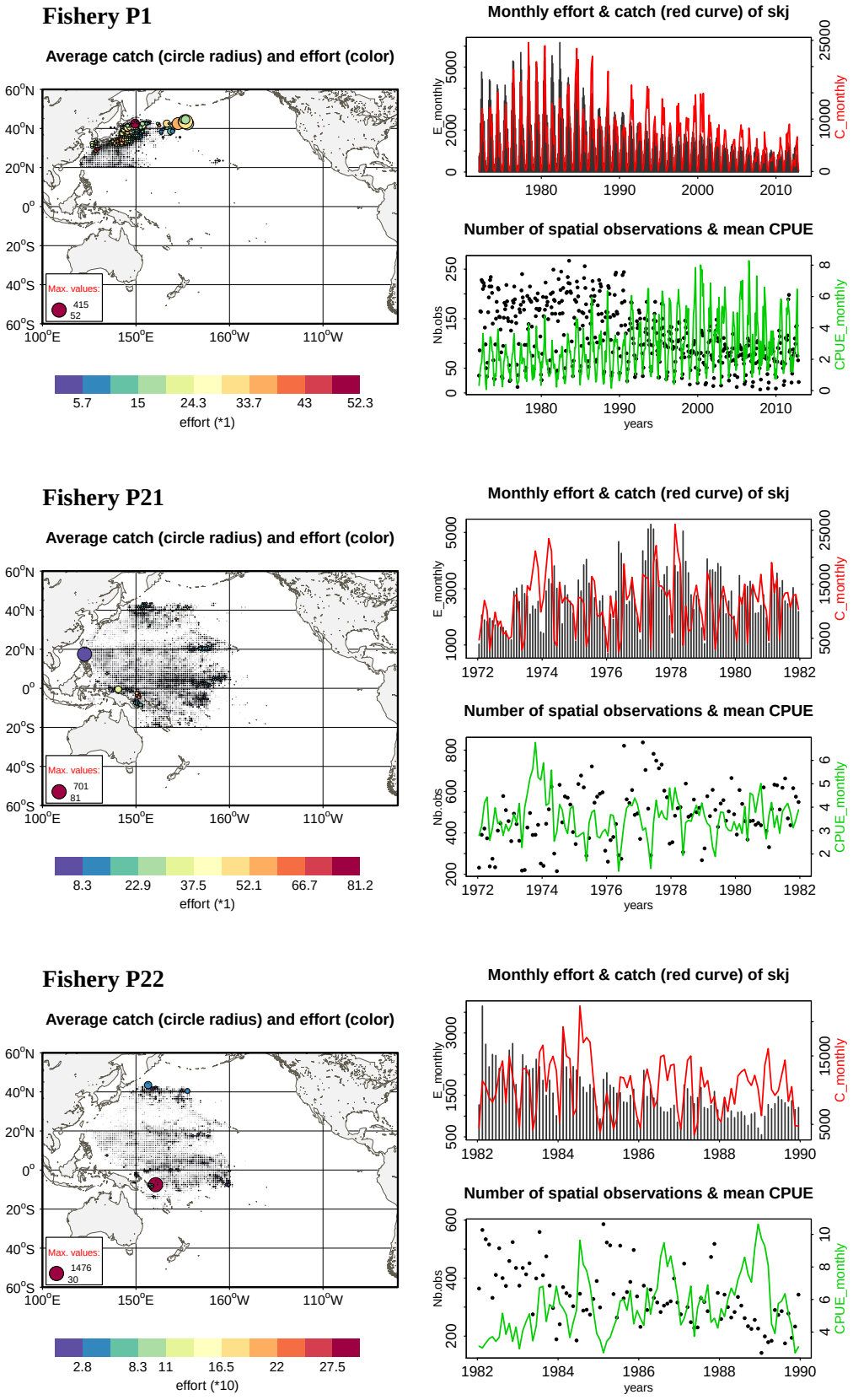

Figure 28: Spatial fishing dataset (effort and catch) being used in current SEAPODYM configuration

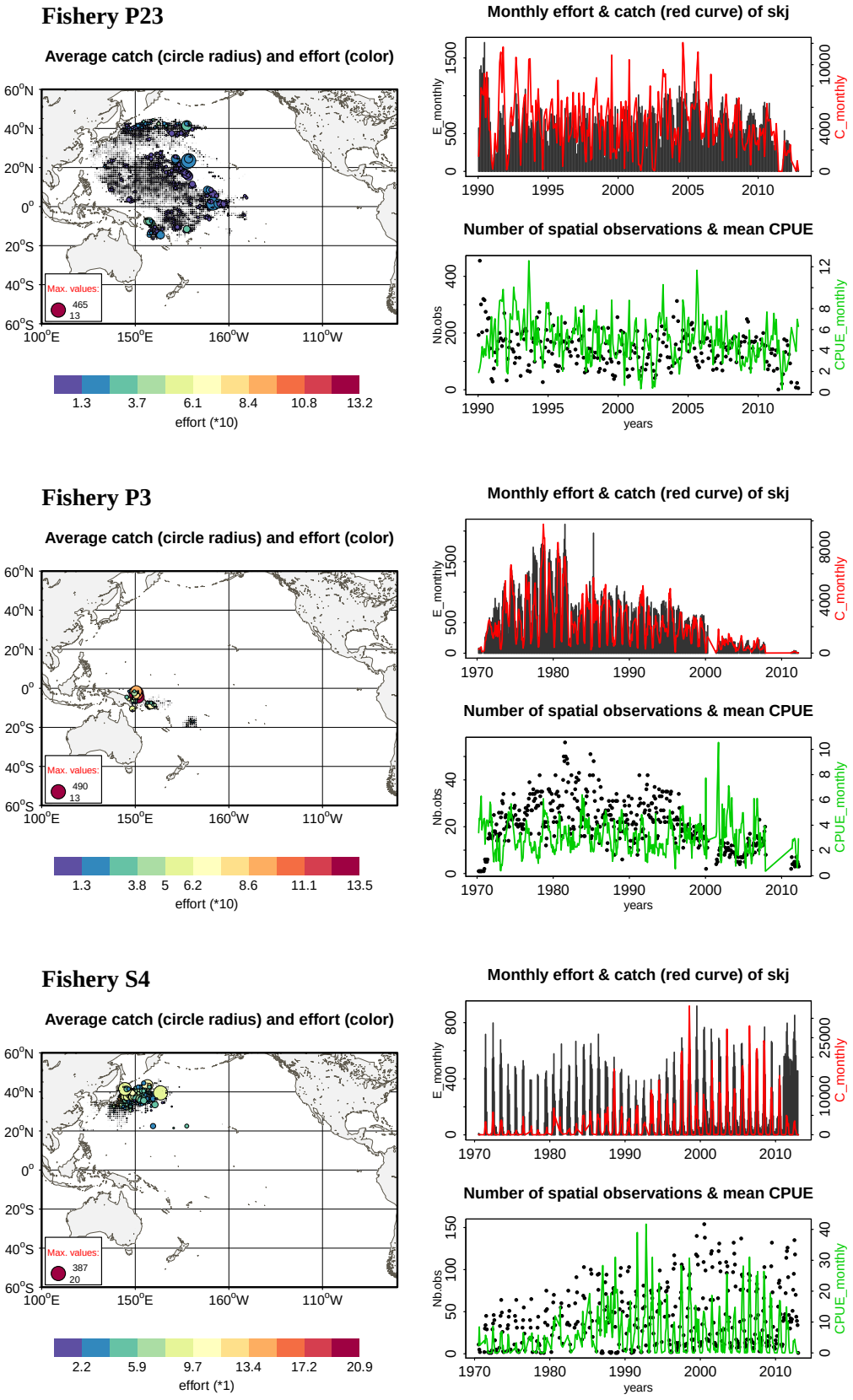

Figure 28: Spatial fishing dataset (effort and catch) being used in current SEAPODYM configuration (Continued)

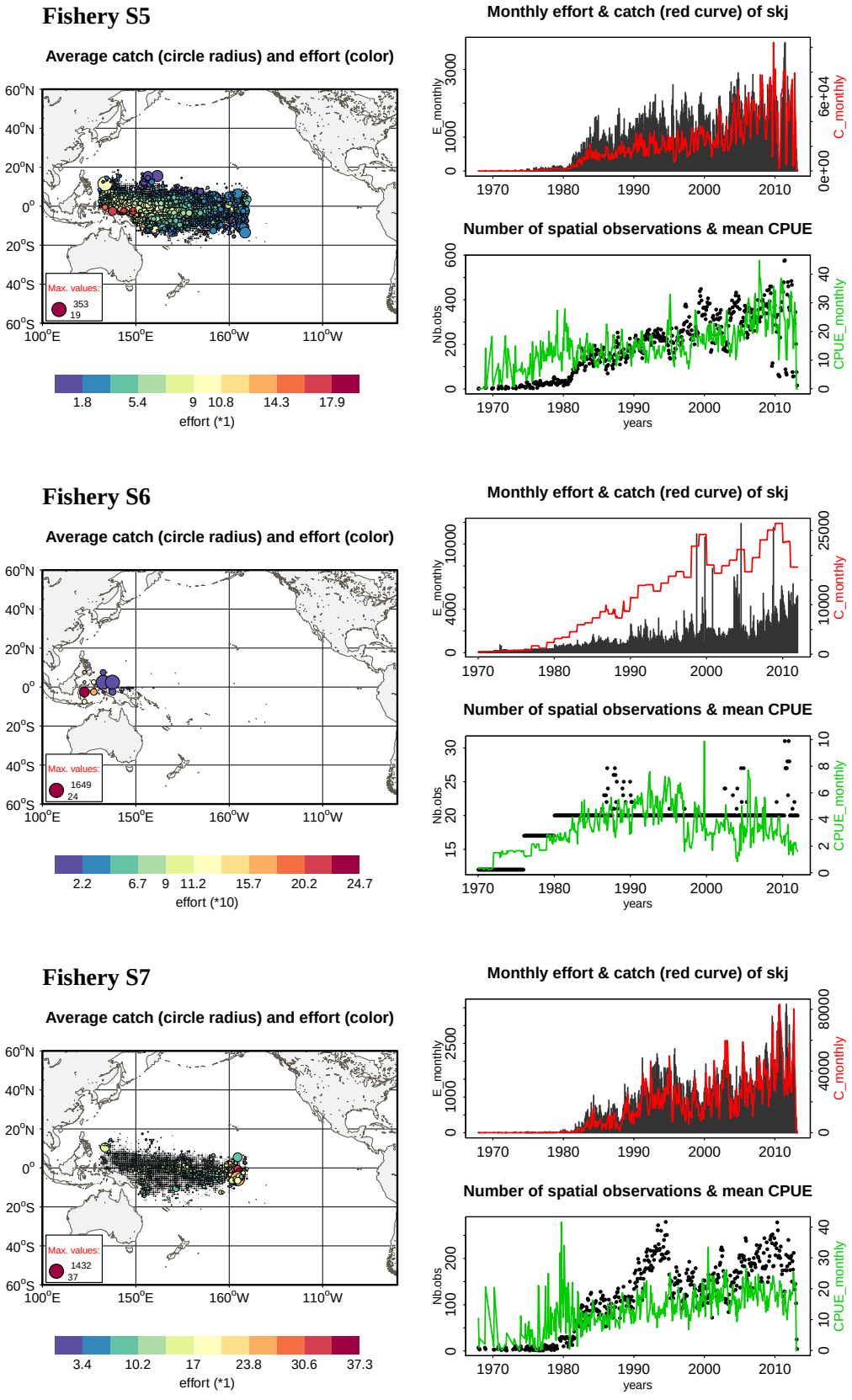

Figure 28: Spatial fishing dataset (effort and catch) being used in current SEAPODYM configuration (Continued)

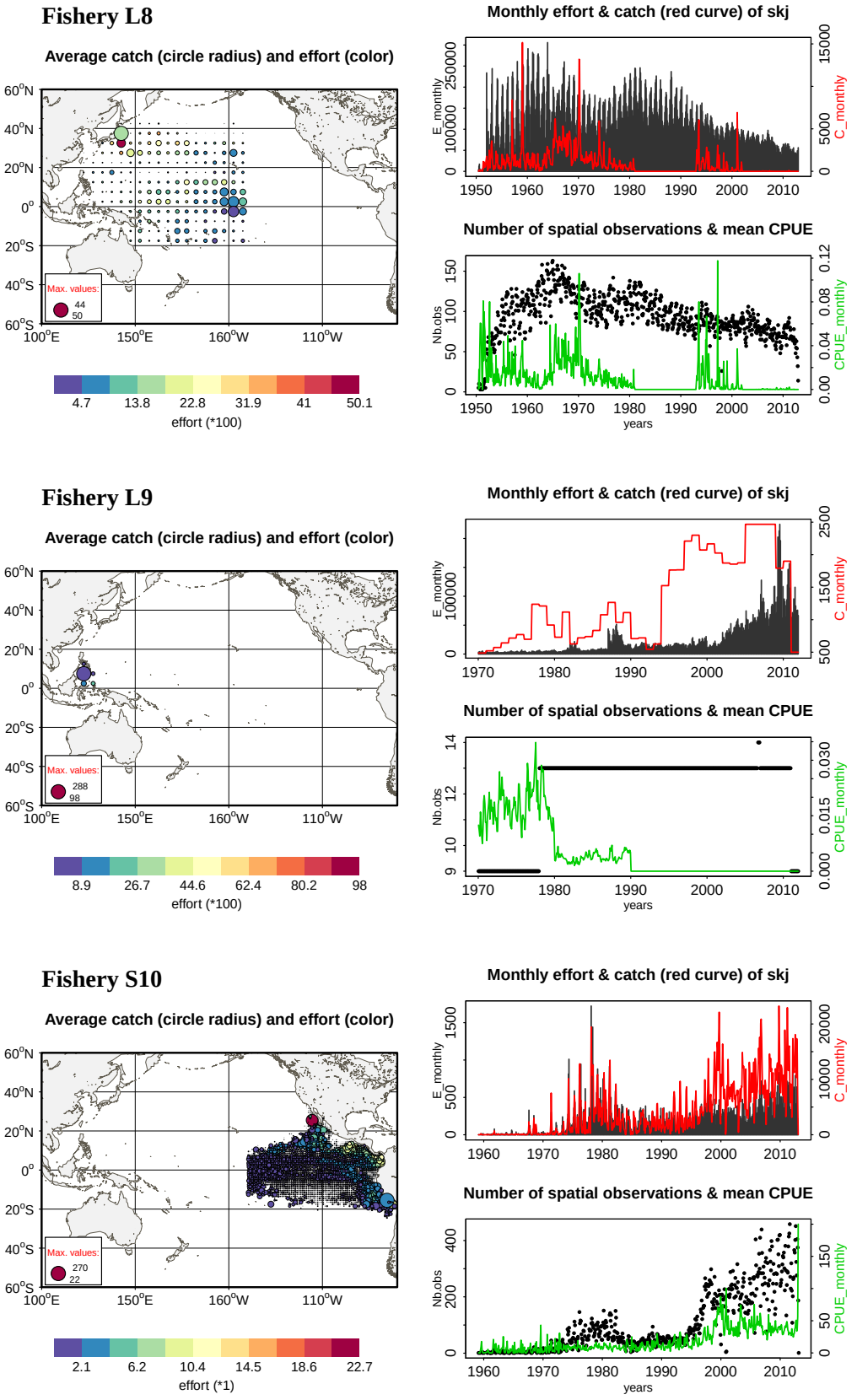

Figure 28: Spatial fishing dataset (effort and catch) being used in current SEAPODYM configuration (Continued)

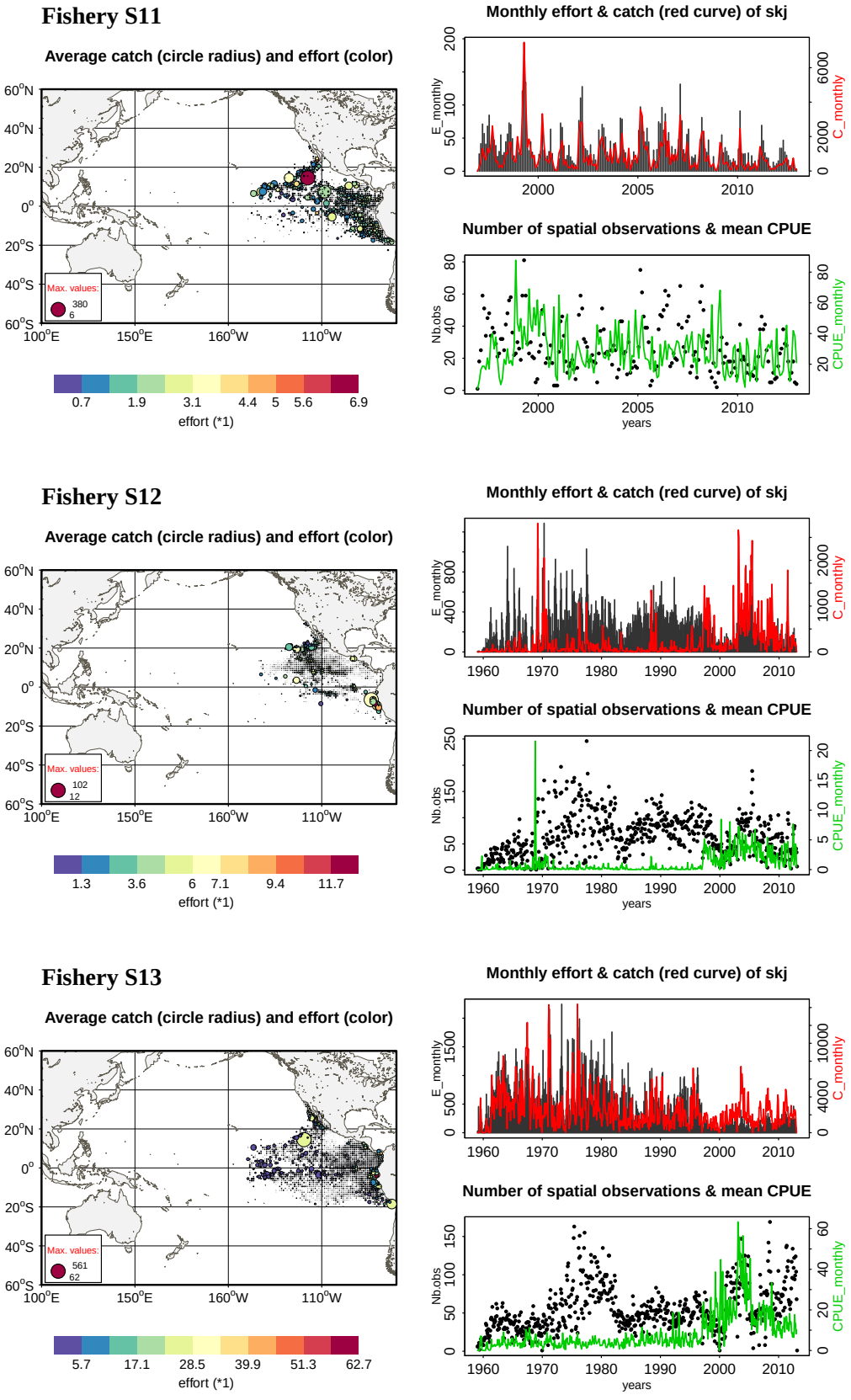

Figure 28: Spatial fishing dataset (effort and catch) being used in current SEAPODYM configuration (Continued)

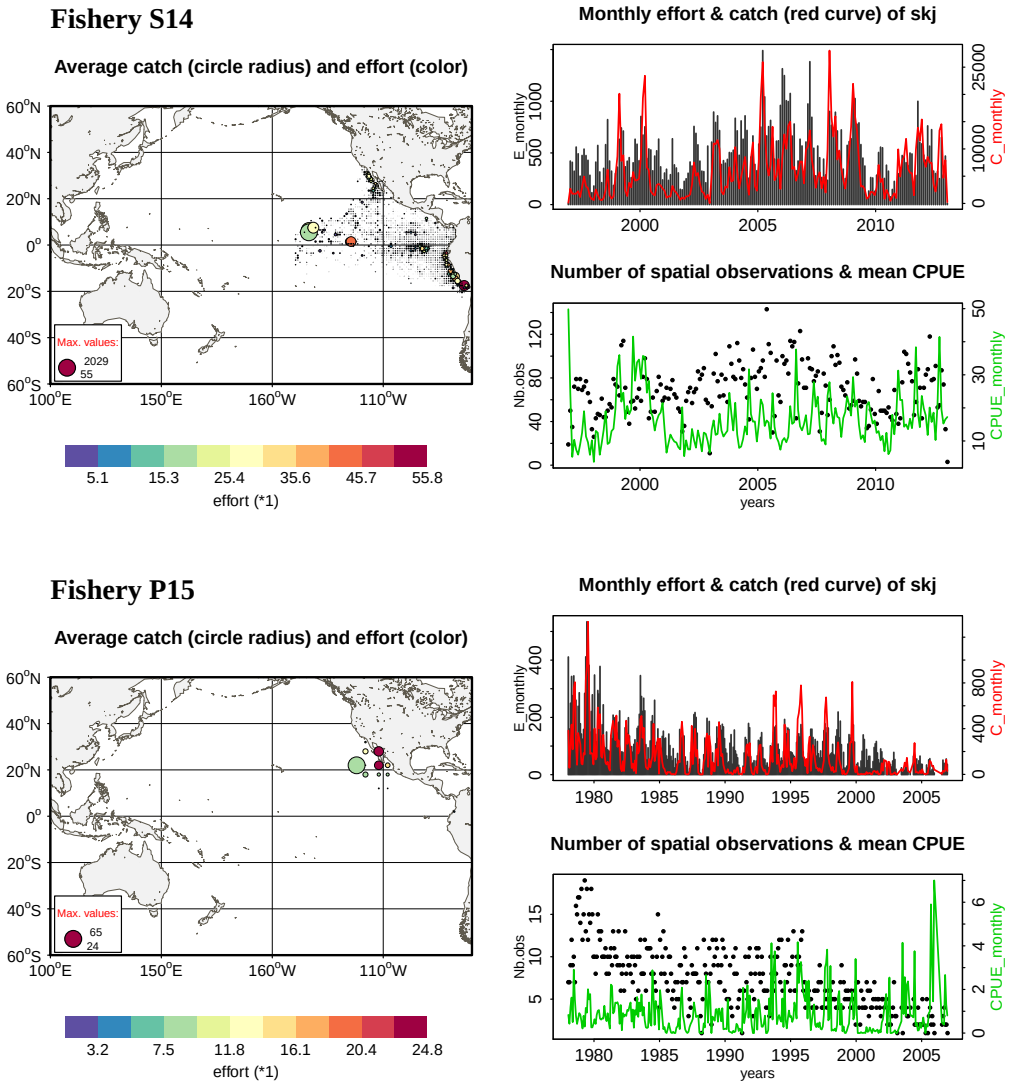

Figure 28: Spatial fishing dataset (effort and catch) being used in current SEAPODYM configuration (Continued)

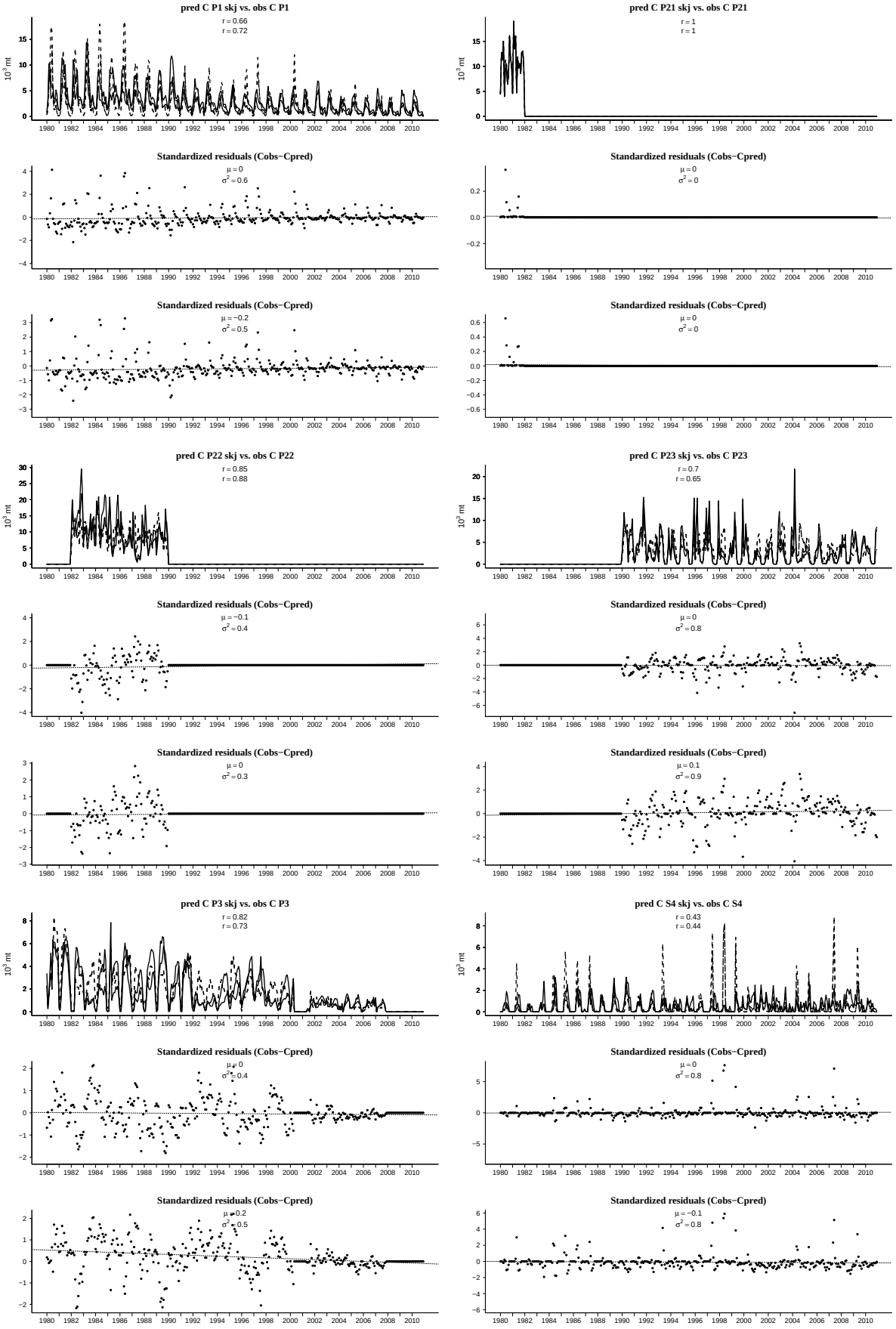

Figure 29: Monthly time series of observed and predicted catch by fishery. Note that catch is predicted based on effort data for all fisheries except P21 and S6 (not included in optimization). The thick line and the first metrics (r and mean and standard deviation for standardized residuals) corresponds to the E3 experiment, the thin line and second metrics are the validation scores of E2 experiments.

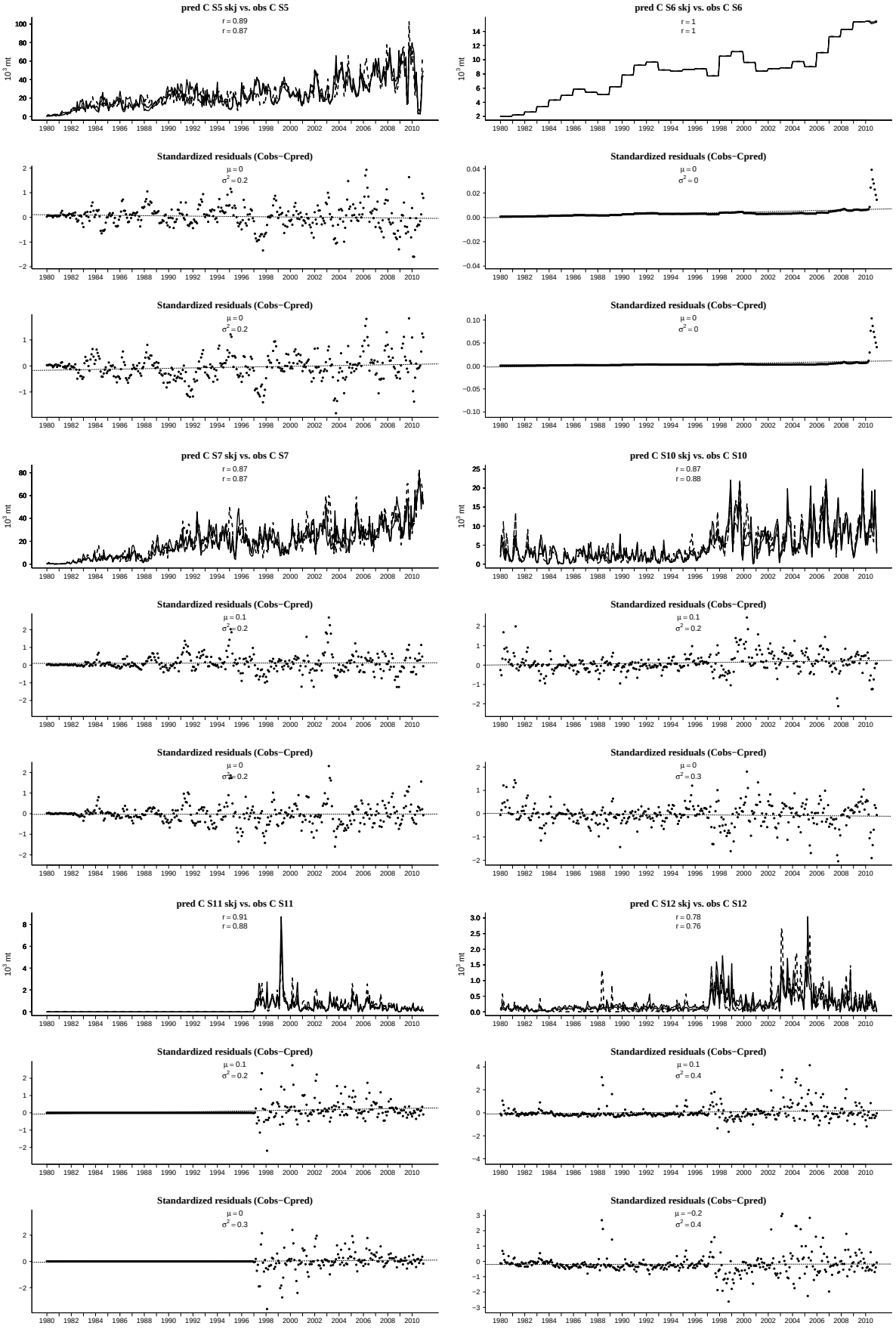

Figure 29: Monthly time series of observed and predicted catch by fishery (Continued)

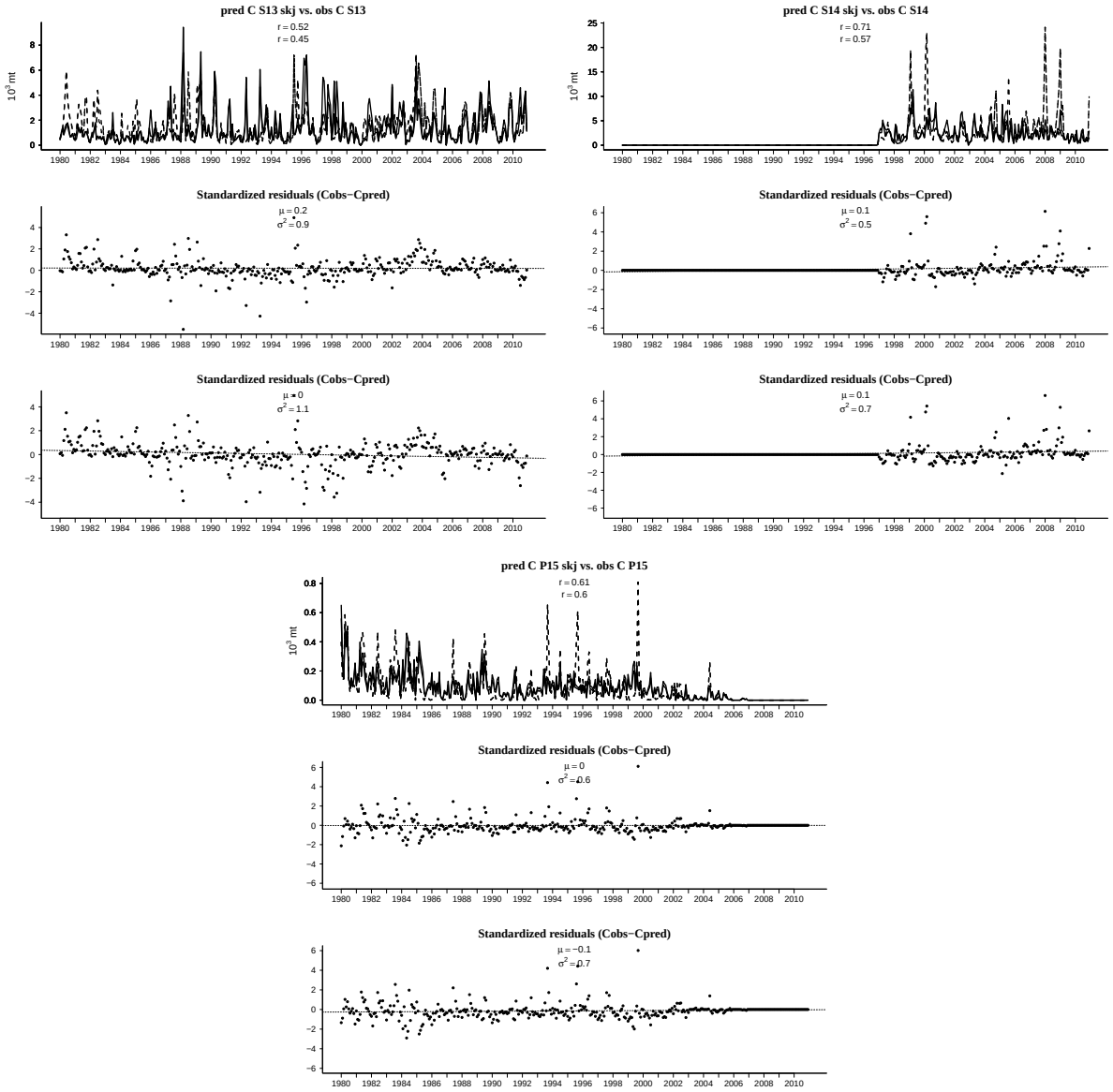

Figure 29: Monthly time series of observed and predicted catch by fishery (Continued)

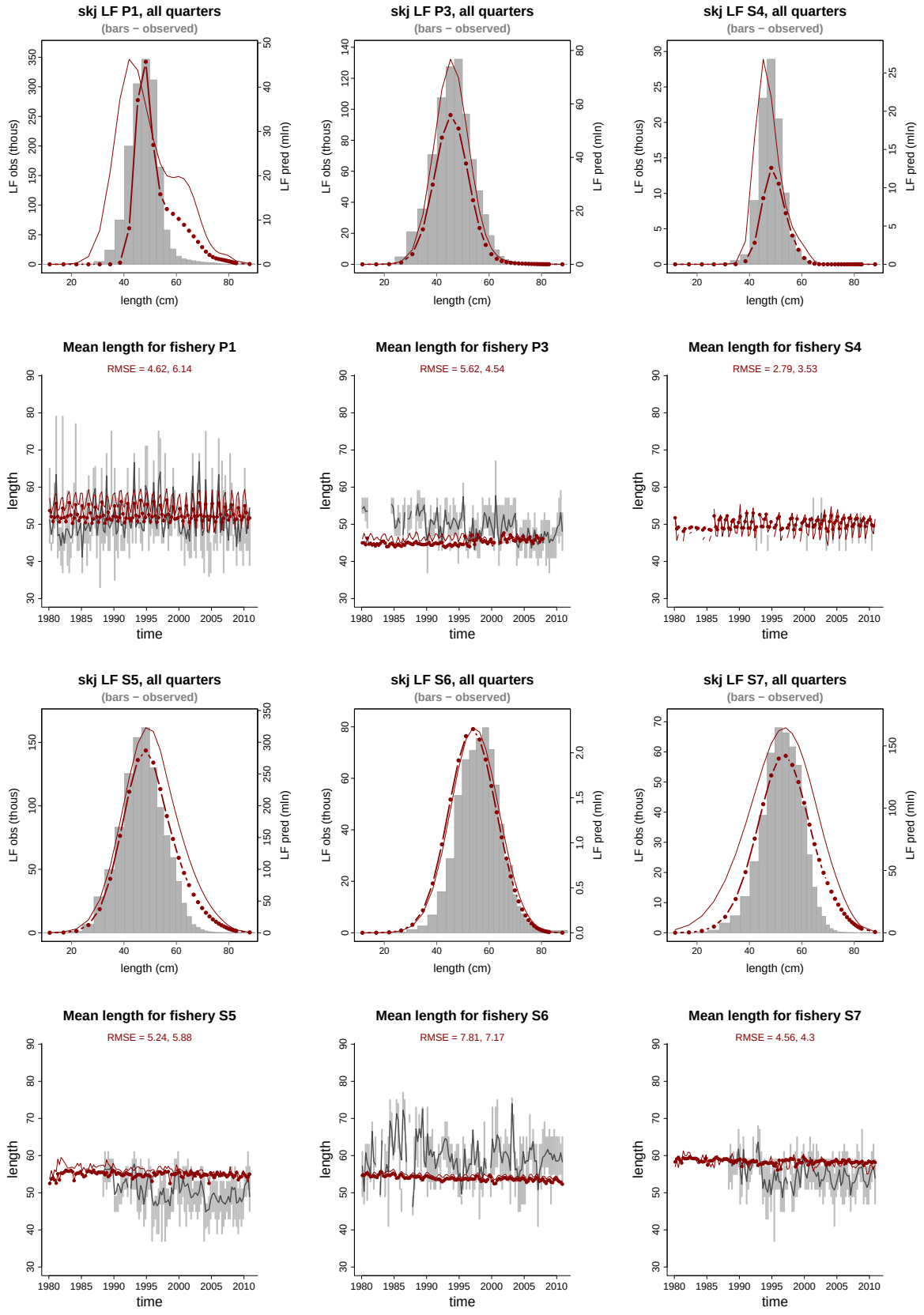

Figure 30: Observed (grey) and predicted (red) length frequencies distribution and mean length in catches. The thick lines and the first metrics (r and mean and standard deviation for standardized residuals) corresponds to the E3 experiment, the thin line and second metrics are the validation scores of E2 experiments.

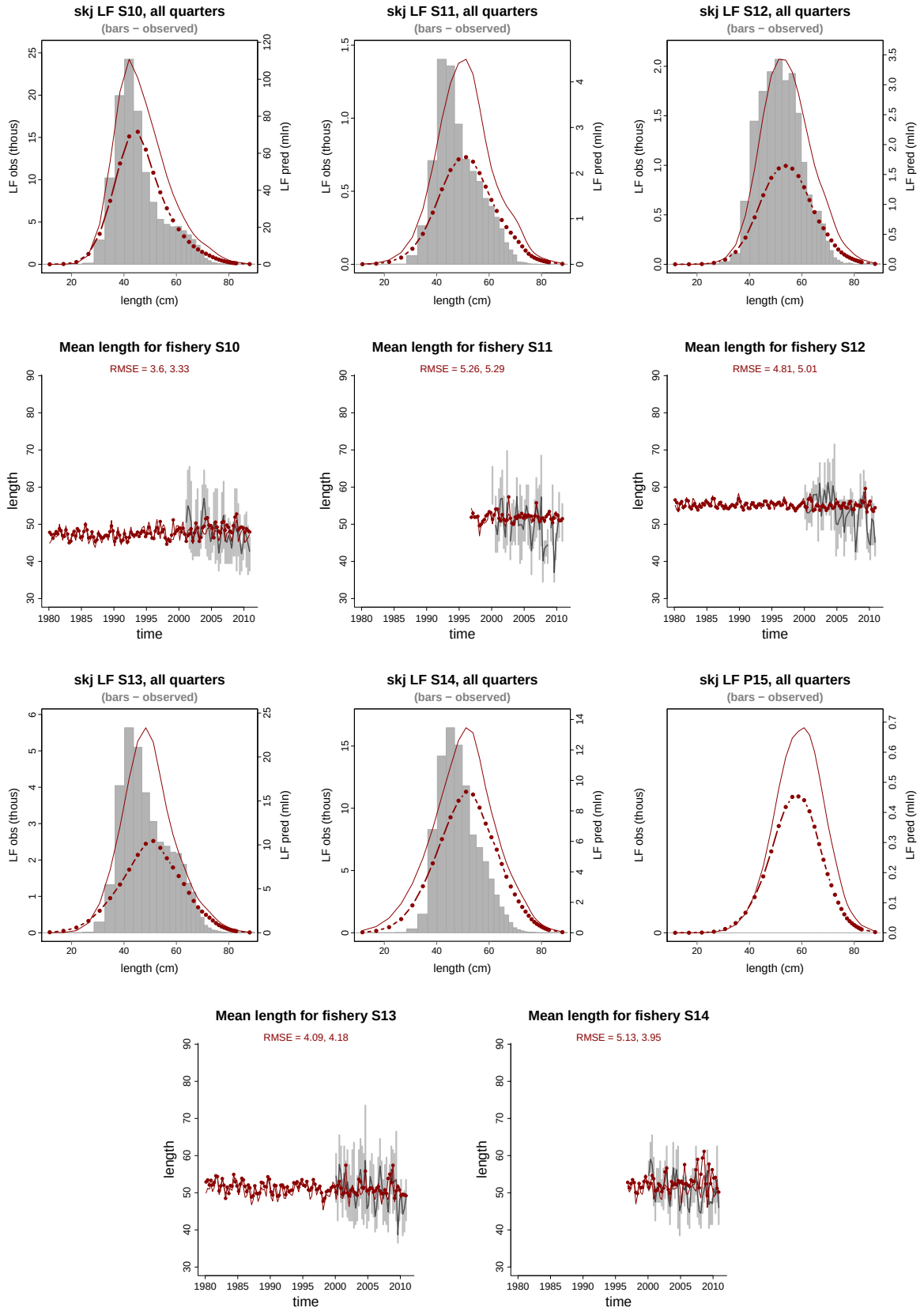

Figure 30: Fit for the length frequencies data. Continued.

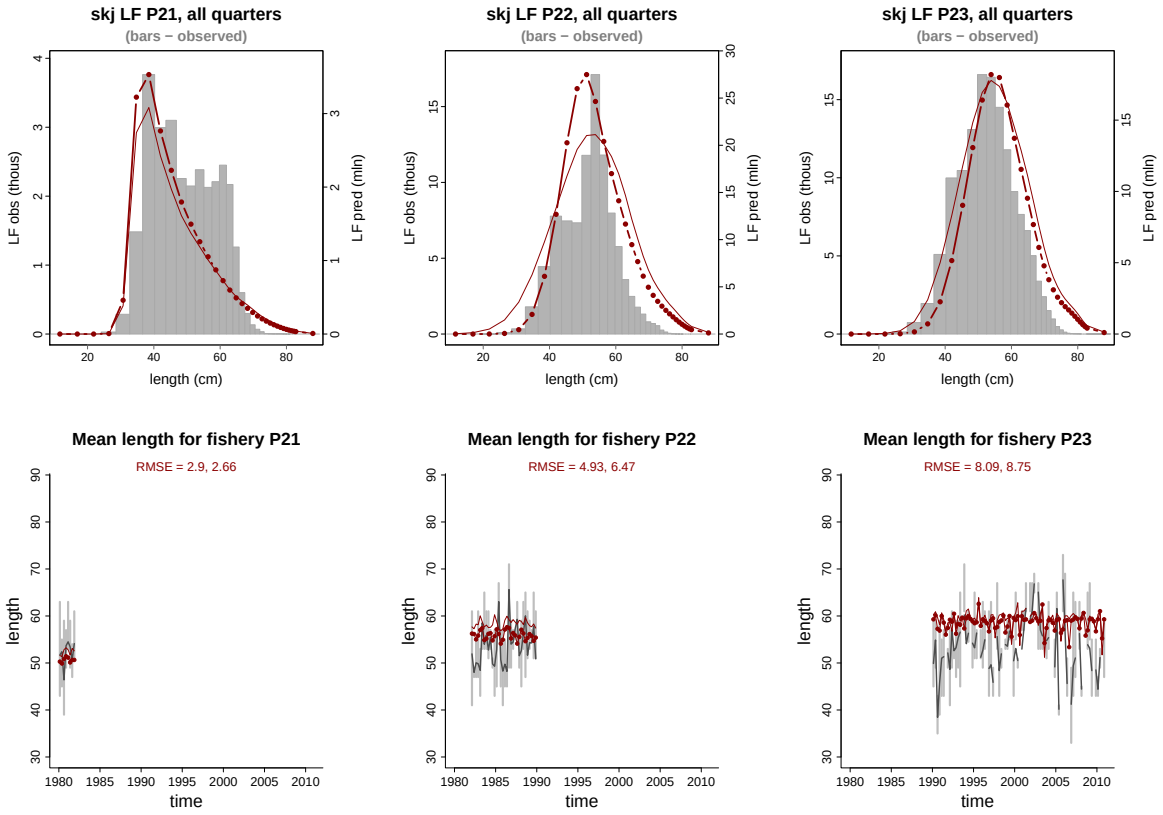

Figure 30: Fit for the length frequencies data. Continued.

References

[Boyce *et al.*, 2008] Boyce, D. G., Tittensor, D. P., Worm B. 2008. Effects of temperature on global patterns of tuna and billfish richness. *Mar. Ecol. Prog. Ser.* 355: 267276. doi: 10.3354/meps07237

[Boehlert and Mundy, 1994] Boehlert G.W. and Mundy, B. C. 1994. Vertical and onshore-offshore distributional pattern of tuna larvae in relation to physical habitat features. *Mar. Ecol. Prog. Ser.* 107: 1-13pp.

[Brill, 1994] Brill, R. 1994. A review of temperature and oxygen tolerance studies of tunas pertinent to fisheries oceanography, movement models and stock assessments. *Fisheries Oceanography* 3:3, 204-216.

[Cayre, 1991] Cayre, P. 1991 Behavior of yellowfin tuna (Thunnus albacares) and skipjack tuna (Katsuwonus pelamis) around fish aggregating devices (FADs) in the Comoros Islands as determined by ultrasonic tagging. Aquat Living Resour 4:112

[WCPFC, 2008] The Commission for the Conservation and Management of Highly Migratory Fish Stocks in the Western and Central Pacific Ocean. Fifth Regular Session, 8-12 December 2008, Busan, Korea: Western and Central Pacific Fisheries Commission, 2008. 206 pp.

[Faugeras and Maury, 2005] Faugeras, B. Maury, O. 2005. An advection-diffusion-reaction population dynamics model combined with a statistical parameter estimation procedure: application to the Indian skipjack tuna fishery. *Mathematical biosciences and engineering* 2: 4, 1-23.

[Graham and Dickson, 2004] Graham, J. B., Dickson, K. A. 2004. Tuna comparative physiology. *The Journal of Experimental Biology* 207: 4015-4024. doi:10.1242/jeb.01267

[Hampton and Fournier, 2001] Hampton, J., Fournier, D. A spatially disaggregated, length-based, age-structured population model of yellowfin tuna (Thunnus albacares) in the western and central Pacific Ocean. Mar. Freshwater Res., 2001, 52, 937963.

[Itano and Holland, 2000] Itano D. G., Holland, K. N. 2000. Movement and vulnerability of bigeye (Thunnus obesus) and yellowfin tuna (*Thunnus albacares*) in relation to FADs and natural aggregation points. *Aquat. Living Resour.* 13: 213223.

[Itano, 2000] Itano, D.G. 2000. The reproductive biology of yellowfin tuna (Thunnus albacares) in Hawaiian waters and the western tropical Pacific Ocean: project summary. SOEST 00-01 JIMAR Contribution 00-328. Pelagic Fisheries Research Program, JIMAR, University of Hawaii.

[Rice *et al.*, 2014] Rice, J., Harley, S., Davies, N. and J. Hampton. 2014. Stock assessment of skipjack tuna in the Western and Central Pacific Ocean. Scientific Committee tenth regular session. Majuro, Republic of the Marshall Islands. 6-14 August 2014. WCPFC-SC10-2014/SA-WP-05

[Lehodey *et al.*, 2009] Lehodey P., Senina I. 2009. An update of recent developments and applications of the SEAPODYM model. 5th Regular Session of the Scientific Committee of the Western Central Pacific Fisheries commission, WCPFC-SC5-2009/EB-WP-10.

[Lehodey *et al.*, 1997] Lehodey, P., Bertignac, M., Hampton, J., Lewis, A., Picaut, J. 1997. El Niño Southern Oscillation and tuna in the western Pacific. *Letters to Nature.* 389, 715-718.

[Lehodey, 2001] Lehodey, P. 2001. The pelagic ecosystem of the tropical Pacific Ocean: dynamic spatial modeling and biological consequences of ENSO. *Progress in Oceanography.* 49, 439-468.

[Lehodey *et al.*, 2003] Lehodey, P., Chai, F., Hampton, J. 2003. Modelling climate-related variability of tuna populations from a coupled ocean biogeochemical-populations dynamics model. *Fish. Oceanogr.* 12: 4/5, 483-494.

[Lehodey, 2004a] Lehodey, P. 2004a. A Spatial Ecosystem And Populations Dynamics Model (SEAPODYM) for tuna and associated oceanic top-predator species: Part I Lower and intermediate trophic components. 17th meeting of the Standing Committee on Tuna and Billfish, Majuro, Republic of Marshall Islands, 9-18 Aug. 2004, Oceanic Fisheries Programme, Secretariat of the Pacific Community, Noumea, New Caledonia, Working Paper: ECO-1: 26 pp. http://www.spc.int/OceanFish/Html/SCTB/SCTB17/ECO-1.pdf

[2004b] Lehodey, P. 2004b. A Spatial Ecosystem And Populations Dynamics Model (SEAPODYM) for tuna and associated oceanic top-predator species: Part II Tuna populations and fisheries. 17th meeting of the Standing Committee on Tuna and Billfish, Majuro, Republic of Marshall Islands, 9-18 Aug. 2004, Oceanic Fisheries Programme, Secretariat of the Pacific Community, Noumea, New Caledonia, Working Paper: ECO-2: 36 pp. http://www.spc.int/OceanFish/Html/SCTB/SCTB17/ECO-2.pdf

[Lehodey and Leroy, 1999] Lehodey, P. and B. Leroy. 1999. Age and growth of yellowfin tuna (*Thunnus albacares*) from the western and central Pacific Ocean as indicated by daily growth increments and tagging data. WP YFT-2, SCTB 12, Papeete, French Polynesia, 16-23 June 1999.

[Lehodey et al, 2014] Lehodey, P., Senina, I., Titaud, O., Calmettes, B., Conchon, A., Dragon, A., Nicol, S., Caillot, S., Hampton, J., Williams, P. 2014. Project 62: SEAPODYM applications in WCPO. WCPFC-SC10-2014/EB-WP-02. 6-14 August, Majuro, Republic of the Marshall Islands.

[Lehodey et al., 2015] Lehodey, P., I. Senina, S. Nicol and J. Hampton. 2015. Modelling the impact of climate change on South Pacific albacore tuna. Deep-Sea Research Part II. Topical Studies in Oceanography, Volume 113.

[Morel and Berthon, 1989] Morel, A, J-F Berthon. 1989. Surface pigments, algal biomass profiles, and potential production of the euphotic layer: Relationships reinvestigated in view of remote-sensing applications. *Limnol. Oceanogr.*, Volume 34: 1545-1562.

[Nicol et al, 2014] Nicol,S., Dessert, M., Gorgues, T., Aumont, O., Menkes, C., P. Lehodey. 2014. Progress report on climate simulations. WCPFC-SC10-2014/EB-IP-02. S.

[Otter Research Ltd, 1994] Otter Research Ltd. 1994. Autodif: a C++ array extension with automatic differentiation for use in nonlinear modeling and statistics. Otter Research Ltd: Nanaimo, Canada.

[Schaefer *et al*, 2011] Schaefer, K. M., Fuller, D. W. Block, B. A. 2011. Movements, behaviour, and habitat utilization of yellowfin tuna (*Thunnus albacares*) in the Pacific Ocean off Baja California, Mexico, determined from archival tag data analyses, including unscented Kalman filtering. *Fisheries Research* 112: 22 - 37.

[Senina *et al.*, 2008] Senina I.N., Sibert, J.R., Lehodey P. 2008. Parameter estimation for basin-scale ecosystem-linked population models of large pelagic predators: Application to skipjack tuna. *Progress in Oceanography* 78, 319-335.

[Senina *et al.*, 2015] Senina, I., Borderies, M., Lehodey, P., 2015. A spatio-temporal model of tuna population dynamics and its sensitivity to the environmental forcing data. Applied Discrete Mathematics and Heuristic Algorithms 1(3), 520. http://dx.doi.org/10.1139/cjfas-2014-0338.

[Schaefer, 2001] Schaefer K.M. 2001 Assessment of skipjack tuna (Katsuwonus pelamis) spawning activity in the eastern Pacific Ocean. Fish Bull 99:343350.

[Sibert *et al.*, 1999] Sibert, J.R., Hampton, J., Fournier, D.A., Bills, P.J. 1999. An advection-diffusion-reaction model for the estimation of fish movement parameters from tagging data, with application to skipjack tuna (*Katsuwonus pelamis*). *Can. J. Fish. Aquat. Sci.* 56, 925-938.

[Sibert *et al.*, 2006] Sibert, J., Hampton, J., Kleiber, P., Maunder, M. 2006. Biomass, Size, and Trophic Status of Top Predators in the Pacific Ocean. Science 314: 1773-1776.

[Sibert and Hampton, 2003] Sibert, J., Hampton, J. 2003. Mobility of tropical tunas and the implications for fishery management. *Marine Policy* 27: 87-95.

[SPC Yearbook 2012] Tuna Fisheries Yearbook. 2012. Western and Central Pacific Fisheries Commission, Pohnpei, Federated States of Micronesia. 148 pp.

[Sund et al., 1981] Sund, P.N., Blackburn, M., Williams, F. 1981. Tunas and their environment in the Pacific Ocean: a review. Oceanogr Mar Biol Ann Rev 19:443512.

[Wexler *et al.*, 2011] Wexler J, Margulies D, Scholey V. 2011. Temperature and dissolved oxygen requirements for survival of yellowfin tuna, Thunnus albacares, larvae. J Exp Mar Biol Ecol 404:6372.

[Williams and Terawasi, 2014] Williams P., Terawasi P. (2014). Overview of tuna fisheries in the Western Central Pacific Ocean, including economic conditions - 2013. 10th Regular Session of the Scientific Committee of the Western Central Pacific Fisheries

commission Majuro, Republic of the Marshall Islands, 6-14 August 2014. WCPFC-SC10-2014/GN WP-1.

[Yamanaka, 1990] Yamanaka, K.L. 1990. Age, growth and spawning of yellowfin tuna in the southern Philippines. IPTP. IPTP Working Paper 21, 1-87.